



Deliverable 7.9: HITEC – Small and mid-scale laboratory experiments

Work Package 7

The project leading to this application has received funding from the European Union's Horizon 2020 research and innovation programme under grant agreement No 847593.



Document information

| | |
|-----------------------------|---|
| Project Acronym | EURAD |
| Project Title | European Joint Programme on Radioactive Waste Management |
| Project Type | European Joint Programme (EJP) |
| EC grant agreement No. | 847593 |
| Project starting / end date | 1st June 2019 – 30 May 2024 |
| Work Package No. | 7 |
| Work Package Title | Influence of Temperature on Clay-based Material Behaviour |
| Work Package Acronym | HITEC |
| Deliverable No. | 7.9 |
| Deliverable Title | HITEC Small and mid-scale laboratory experiments |
| Lead Beneficiary | CIEMAT |
| Contractual Delivery Date | May 2024 |
| Actual Delivery Date | May 2024 |
| Type | Final report of WP7 Task 3.3 |
| Dissemination level | Public |
| Authors | María Victoria Villar (CIEMAT), Jiří Svoboda (CTU), Kateřina Černochová (CTU), Carlos Gutiérrez-Álvarez (CIEMAT), Rubén J. Iglesias(CIEMAT), Guillermo García-Herrera (CIEMAT) |

To be cited as:

Villar, M.V., Svoboda, J., Černochová, K., Gutiérrez-Álvarez, C., Iglesias, R.J., García-Herrera, G. (2023): HITEC Technical Report on small and mid-scale laboratory experiments. Final version as of 23.05.2024 of deliverable D7.9 of the HORIZON 2020 project EURAD. EC Grant agreement no: 847593.

Disclaimer

All information in this document is provided "as is" and no guarantee or warranty is given that the information is fit for any particular purpose. The user, therefore, uses the information at its sole risk and liability. For the avoidance of all doubts, the European Commission has no liability in respect of this document, which is merely representing the authors' view.

Acknowledgement

This document is a deliverable of the European Joint Programme on Radioactive Waste Management (EURAD). EURAD has received funding from the European Union's Horizon 2020 research and innovation programme under grant agreement No 847593.

| Status of deliverable | | |
|-------------------------------|-----------------------------------|------------|
| | By | Date |
| Delivered (Lead Beneficiary) | [CIEMAT] | 10/11/2023 |
| Verified (WP Leader) | [VTT] | 19/05/2024 |
| Reviewed (Reviewers) | Jinsong Liu [SSM] | 29/02/2024 |
| | Michael Holmboe [Umeå University] | 18/05/2024 |
| Approved (PMO) | Bharti Reddy | 23/05/2024 |
| Submitted to EC (Coordinator) | Andra (Coordinator) | 23/05/2024 |

Authors

| Organisation | Authors |
|--------------|--|
| CIEMAT | María Victoria Villar, Carlos Gutiérrez-Álvarez, Rubén J. Iglesias, Guillermo García-Herrera |
| CTU | Jiří Svoboda, Kateřina Černochová |

Executive Summary

CIEMAT and SÚRAO [CTU] performed thermo-hydraulic tests intended to simulate the conditions of the bentonite buffer in the repository. Namely two kinds of tests were performed:

1. hydration tests under thermo-hydraulic gradient (TH tests), and
2. hydration tests under high isothermal temperature.

The first group of tests, in which the buffer material is simultaneously submitted to thermal and hydraulic gradients in opposite directions, aimed to simulate the conditions of the whole barrier during operation, where the temperatures may be significantly different from those areas closest to the canister to those at the host rock contact. These tests were performed using different bentonites (MX-80, Bara-Kade, FEBEX, BCV), cell dimensions (height from 10 to 50 cm, diameter from 7 to 30 cm), initial buffer conditions (powder, pellets, water contents from 6 to 17%, dry density from 0.9 to 1.6 g/cm³) and testing protocols (heating followed by hydration, hydration followed by heating, simultaneous heating and hydration). The tests can be considered medium-scale ones, since their dimensions are relevant for the usual barrier thickness envisaged by most repository concepts. In all of them the heater plate simulating the canister surface was placed at the bottom (at temperatures 140-150°C) and the temperature on top was regulated either at 20°C or at room temperature. Hydration water (deionised, glacial or saline) was supplied through the top at a low injection pressure. Out of the TH tests included in this Subtask, test HEE-B reproduced the conditions of a large-scale in situ experiment (HE-E at Mont Terri), whereas the others were not representative of any particular disposal concept.

The second group of tests aimed at assessing how the high temperatures close to the heater could affect the hydration rate and swelling development. Thus, they were carried out under isothermal high temperatures (120, 140°C) with FEBEX bentonite compacted at dry density 1.6 g/cm³ with its hygroscopic water content.

The tests are described in detail in this report (or in cited published literature) and the results concerning online measurements during operation (temperature, relative humidity, pore pressure, axial and radial mechanical pressures, water intake) and postmortem physical state of the bentonite (water content, dry density) are presented herein. The following conclusions could be reached:

- The testing sequence (heating before or after hydration) impacts the thermo-hydro-mechanical evolution of the system.
- Hydration under thermal gradient can progress even if the water injection pressure is very low, but full saturation may take much longer than under lower isothermal conditions. However, the tests reported did not allow to check if full saturation of the areas closest to the heater is possible, either because the tests were too short or because of experimental artefacts, namely evaporation through the cell sensors' inlets.
- Relevant radial swelling stresses –associated to the increase in water content– were recorded during hydration under high temperature, higher when diluted water was used instead of saline one.
- The postmortem state was linked to the testing protocol:
 - In those tests in which no full saturation was reached (because there was not an initial saturation phase), significant gradients in the water content and dry density distributions developed in the bentonite, with higher water contents close to the hydration surface, where the dry density was lower.
 - Only in the test in which bentonite –with a very low dry density– was first saturated and then heated, the final dry density and water content were homogeneous in most of the bentonite column.
 - In the isothermal tests, where hydration took place through the bottom of the samples, the dry density was lower on the bentonite block side opposite to the hydration surface, where also the highest water contents were measured. This distribution likely results from the upwards vapour movement, which concentrated on top of the cell and would also trigger bentonite swelling and increase in porosity.

- The tests performed with pellets showed trends of behaviour similar to those expected for compacted bentonite.

Table of content

| | |
|---|----|
| Executive Summary..... | 6 |
| Table of content..... | 9 |
| List of figures | 11 |
| List of Tables | 14 |
| 1. Introduction | 15 |
| 2. CIEMAT | 16 |
| 2.1 Introduction | 16 |
| 2.1.1 Material | 16 |
| 2.1.2 Research plan..... | 16 |
| 2.2 Procedures | 19 |
| 2.2.1 Large-scale lab TH cell (HEE-B) | 19 |
| 2.2.2 Medium-scale lab TH cells | 20 |
| 2.2.3 Medium-scale lab cell: infiltration at high T | 21 |
| 2.3 Results..... | 23 |
| 2.3.1 Large-scale lab TH cell (HE-E)..... | 23 |
| 2.3.2 Medium-scale lab TH cells | 27 |
| 2.3.3 Medium-scale lab cells: infiltration at high T..... | 30 |
| 2.4 Conclusion | 32 |
| 3. CTU (SÚRAO) | 33 |
| 3.1 Introduction | 33 |
| 3.1.1 Material | 33 |
| 3.1.2 Research plan..... | 33 |
| 3.2 Procedures | 34 |
| 3.2.1 Laboratory set-up..... | 34 |
| 3.2.2 Preparation of the material | 36 |
| 3.2.3 Experimental procedures..... | 37 |
| 3.3 Results..... | 38 |
| 3.3.1 Test 1 – bentonite powder | 38 |
| 3.3.2 Test 2 – bentonite pellets | 41 |
| 3.3.3 THM analysis | 46 |
| 3.4 Conclusion | 49 |
| 4. Summary and conclusions | 50 |
| References | 52 |

List of figures

| | |
|---|----|
| Figure 2-1. Schematic design of cell HEE-B and sensors with the external insulation (green crosses are temperature external sensor positions) | 19 |
| Figure 2-2. Appearance of the 26 sampling sections of the bentonite column of test HEE-B (hydration zone on the left, the photographs may show deformed diameters along the column which are not real) | 19 |
| Figure 2-3. Longitudinal cross-sections of the HT cells with the sensors installed (in the sensors name, x stands for the cell number, 1 or 2) | 20 |
| Figure 2-4. HT-1 and HT-2 cells wrapped with isolating material during operation | 21 |
| Figure 2-5. Schematic design of the high-temperature oedometer (vertical and horizontal cross-sections) | 22 |
| Figure 2-6. Isothermal cell wrapped in the heating mat and isolating material (left) and placed in the frame with load cell on top (right) | 22 |
| Figure 2-7. Equilibrium values measured inside the material after the heater was set to 100°C (t=3524 h) and 140°C (t=5015 h) in cell HEE-B | 24 |
| Figure 2-8. Average temperatures along the column measured by the sensors inside the cell and external temperatures measured with thermocouples from June 2013 to June 2021 | 24 |
| Figure 2-9. Evolution of water intake and relative humidity in cell HEE-B after the beginning of hydration (sensor 1 placed at 40 cm from the heater, sensor 2 at 22 cm and sensor 3 at 10 cm) | 25 |
| Figure 2-10 Water content and dry density of the column measured at the end of the test HEE-B (empty symbols: estimated from weight and volume). The thick vertical lines indicate the location of sensors, and the dotted horizontal lines the initial values | 26 |
| Figure 2-11 Axial pressure measured on top of cell HEE-B and water intake from the beginning of hydration (left) and relation between relative humidity measured by sensor 1 and axial pressure (right) | 26 |
| Figure 2-12. Time evolution of relative humidity and temperature inside the bentonite during the heating phase of tests HT1 and HT2 | 27 |
| Figure 2-13. Temperatures and relative humidity inside the bentonite at the end of the heating phase of tests HT1 and HT2 | 27 |
| Figure 2-14. Evolution of radial pressure during hydration with glacial water of cell HT1 (PT13 at 2.5 cm from the heater, PT12 at 5 cm and PT11 at 7.5 cm) | 28 |
| Figure 2-15. Evolution of radial pressure during hydration with saline water of cell HT2 (PT23 at 2.5 cm from the heater, PT22 at 5 cm and PT21 at 7.5 cm) | 28 |
| Figure 2-16. Upper part of the block from cell HT2 and material corresponding to the section closest to the heater | 30 |
| Figure 2-17. Final water content (w.c), dry density (d.d.) and degree of saturation along the bentonite block of cell HT2 (~2.5 years of hydration with saline water under a high thermal gradient). The discontinuous horizontal lines indicate the initial values | 30 |
| Figure 2-18. Pressure and water intake evolution in test ET6, isothermal at 120°C (left) and test ET7, isothermal at 140°C (right). The distance to the hydration surface of the radial pressure sensors P1, P2 and P3 is indicated in the legends | 31 |

| | |
|---|----|
| Figure 2-19. Radial and axial (at distance 10 cm) pressures measured in two hydration tests performed under isothermal conditions (FEBEX bentonite compacted at 1.6 g/cm ³ saturated with deionised water) | 31 |
| Figure 2-20. Final distribution of water content and dry density in two hydration tests performed under isothermal conditions (FEBEX bentonite compacted at 1.6 g/cm ³ saturated with deionised water)..... | 32 |
| Figure 3-1. Schema of medium-scale laboratory experiment | 34 |
| Figure 3-2. Schematic illustration of saturation system of medium-scale laboratory experiment | 35 |
| Figure 3-3. The experiment set-up | 35 |
| Figure 3-4. Schema of the instrumentation of medium-scale laboratory experiment..... | 36 |
| Figure 3-5. Evolution of parameters of medium-scale laboratory experiment – Test 1 (powder) | 39 |
| Figure 3-6 Sampling plan for dismantling of Test 1 | 40 |
| Figure 3-7. Distribution of dry density and degree of saturation as a function of the distance from the heater at the end of Test 1 | 40 |
| Figure 3-8. Evolution of parameters of medium-scale laboratory experiment – Test 2 (bentonite pellets) | 42 |
| Figure 3-9. Sampling points for the determination of water content and dry density in layers of Test 2 | 43 |
| Figure 3-10. Distribution of final water content as a function of the vertical distance from the heater at each sampling point from the centre through the middle (75 mm from centre) to the edge (150 mm from the centre) in Test 2..... | 44 |
| Figure 3-11. Distribution of final degree of saturation as a function of the distance from the heater at each sampling point from the centre through the middle (75 mm from centre) to the edge (150 mm from the centre) in Test 2..... | 44 |
| Figure 3-12 Distribution of final dry density as a function of the distance from the heater at each sampling point from the centre through the middle (75 mm from centre) to the edge (150 mm from the centre) in Test 2..... | 45 |
| Figure 3-13. Average final dry density and degree of saturation in each layer in Test 2 (pellets) | 46 |
| Figure 3-14. Temperature inside the bentonite as a function of the distance from the heater and on the lid. Comparison of temperature evolution with powdered bentonite and pellets. Thermometer record 60 mm from the centre of the experiment – slight influence of ambient temperature. Room temperature: 18.8°C..... | 47 |
| Figure 3-15. Temperature inside the bentonite as a function of the distance from the heater and on the lid. Comparison of temperature evolution with powdered bentonite and pellets. Thermometer record 120 mm from the centre of the experiment – Edge of the experiment, significant effect of ambient temperature. Room temperature: 18.8°C..... | 47 |
| Figure 3-16. Comparison of the degree of saturation at the end of Test 1 (powdered bentonite with a dry density of 940 kg/m ³) and Test 2 (pelletized bentonite with a dry density of 1408 kg/m ³)..... | 48 |

List of Tables

| | |
|---|----|
| <i>Table 2-1. CIEMAT - Large-scale lab TH cell (HEE-B)</i> | 17 |
| <i>Table 2-2. CIEMAT – Medium-scale lab TH cell (Bara-Kade)</i> | 18 |
| <i>Table 2-3. CIEMAT – Medium-scale lab cell: infiltration at high T</i> | 18 |
| Table 2-4. Characteristics of the tests performed in the high-temperature oedometer (ET_1 to ET5 were trial tests, ET_8 failed) | 22 |
| <i>Table 3-1. CTU – Medium-scale laboratory tests</i> | 33 |
| <i>Table 3-2. Main characteristics of the samples in Test 1 and Test 2 after installation</i> | 37 |
| <i>Table 3-3. Key phases of Test 1</i> | 38 |
| <i>Table 3-4. Key phases of Test 2</i> | 38 |
| <i>Table 4-1. Summary of the TH performed in Subtask 3.3</i> | 50 |

1. Introduction

The overall objective of WP HITEC was to evaluate whether an increase of temperature is feasible and safe by applying existing and the within-the-task newly produced knowledge about the behaviour of clay buffer materials at elevated temperatures. Inside this WP, Task 3 includes the experimental work carried out in buffer materials. The objectives of Task 3 subtasks were defined as:

- Assessment of the impact of having clay buffer subjected to high temperatures over long time periods on the clay buffer properties (Subtask 3.1, with results reported in D7.7.)
- Determination of bentonite hydro-mechanical properties for temperatures higher than 100°C, which will provide parameters for the modelling work (Subtask 3.2, with results reported in D7.8.)
- Identification of key processes at high temperature, particularly those affecting the saturation rate, because this will condition the time the buffer is in dry conditions and under high temperature (Subtask 3.3, with results reported in D7.9.)
- Calibration and development of suitable THM models for clay buffer at higher temperatures, using the information provided by the tests in Subtask 3.3, to which this activity also belongs. The results have been reported in D7.10.

The tests in Subtask 3.3, to which this report refers, were designed to simulate the conditions of the barrier material during operation, when it is simultaneously subjected to opposite thermal and hydraulic gradients. High temperatures at the canister surface may result in strong evaporation near the heater and vapour movement towards the external part of the buffer. As a consequence, part of the barrier, or all of it, depending on the particular disposal concept, will remain unsaturated and under high temperatures during periods of time that can be very long. One of the concerns about the behaviour of the bentonite barrier is the preservation of its good mechanical properties after being intensely dried in the conditions of the repository. The tests included in this Subtask aimed at assessing how the temperature gradient may actually impact the hydration rate and consequently the time that part of the barrier will remain unsaturated. In these thermo-hydraulic (TH) tests performed in cylindrical cells, the sealing material is subjected simultaneously to heating and hydration in opposite directions, in order to simulate the conditions of the clay barrier in the repository, i.e. the interaction of the water coming from the host rock and the thermal gradient generated by the heat emitted by the wastes in the canisters. Usually the TH cells are instrumented, and they provide online information about the changes in temperature, relative humidity and pressure inside the buffer, as well as of the water intake rate. At the end of the experiments the final state of the bentonite in terms of porosity and water content can be assessed through detailed subsampling of the buffer column. All this information is very useful for the calibration and validation of THM models (as reported in D7.10). Additionally, the mineralogy, geochemistry and THM properties of the treated material may be determined in postmortem tests and compared with those of the original material (Subtask 3.1, D7.7).

This document describes the work carried out and results obtained for the experimental work of Subtask 3.3 by CIEMAT and CTU. The subsequent chapters provide this information for the different participants and a summary of the findings is provided at the end of the report.

2. CIEMAT

2.1 Introduction

The thermo-hydraulic tests conducted by CIEMAT aimed at simulating in the laboratory the conditions of barrier materials during operation. These tests provide online and postmortem results that are very useful for the verification and validation of models of THM behaviour. Two kinds of tests were performed: hydration tests under thermohydraulic gradient (TH tests) and hydration tests under high isothermal temperature. Out of the TH tests included in this Subtask, one of them reproduced the conditions of a large-scale in situ experiment (HE-E at Mont Terri), and was running since 2012. Two new TH tests started in the framework of HITEC and have been running with the heaters set at 150°C.

2.1.1 Material

Three different materials were used in the tests: MX-80 bentonite pellets, Bara-Kade bentonite powder and FEBEX bentonite.

2.1.1.1 MX-80 bentonite

From Wyoming (USA), produced by American Colloid Co. It is a bentonite of volcanic origin, powdered and Na-homogenised. The pellets used were received from Mont Terri and are the same as those used in the HE-E in situ experiment ([1]). They are irregular pellets of size <10 mm, dry density 2.75 g/cm³ and water content 6%.

The content of montmorillonite in the MX-80 bentonite is between 65 and 90% (depending on the batch), with quartz, plagioclase and K-feldspars (contents between 4 and 15%), and minor quantities of cristobalite, tridymite, calcite, gypsum, pyrite, illite. Na⁺ is the main exchangeable cation (50-74 meq/100 g), with also Ca²⁺ (10-30 meq/100 g) and Mg²⁺ (3-8 meq/100g) ([2], [3], [1]).

2.1.1.2 Bara-Kade bentonite

The material with commercial name 'Bara-Kade' is Wyoming sodium bentonite similar to MX-80. Its use was proposed by Posiva in June 2020, although it had not been initially foreseen. The as-received water content was 8.2%.

2.1.1.1 FEBEX bentonite

It is a 900-t batch prepared in 1996 coming from the Cortijo de Archidona quarry (Cabo de Gata area, SE Spain). On site it was homogenised, air-dried and volcanic pebbles were manually removed. At the factory the processing consisted in crumbling, drying in a rotary oven at temperatures between 50 and 60°C and sieving through a 5-mm mesh.

More than 90% is a montmorillonite-illite mixed layer (with 10-15% of illite layers), with variable quantities of quartz (2±1%), plagioclase (3±1%), K-felspar (traces), calcite (1±1%), and cristobalite-trydimite (2±1%). Ca²⁺ (33±2 meq/100 g), Mg²⁺ (33±3 meq/100 g) and Na⁺ (28±1 meq/100 g) are the main exchangeable cations. The main soluble ions are sodium and chloride ([4]). Other THM properties can be found in [5].

2.1.2 Research plan

Since three different kinds of TH tests were proposed, the research plan is presented in separate tables, one for each kind of test.

Table 2-1. CIEMAT - Large-scale lab TH cell (HEE-B)

| |
|---|
| <p>2.1.2.1 Material (BoM item):</p> <p>MX-80 pellets</p> |
| <p>2.1.2.2 Material treatment (sample preparation for test and loading procedure):</p> <p>The pellets, with a water content of 6.4%, were poured into the cell and slightly vibrated to give an overall dry density $\sim 1.5 \text{ g/cm}^3$</p> |
| <p>2.1.2.3 Temperature (to which material was/will be exposed to) and exposure time</p> <p>Heater $T=140^\circ\text{C}$, with a sharp gradient close to the heater and temperatures close to the room ones on the opposite side. Heating lasted for 10 years.</p> |
| <p>2.1.2.4 Tests carried out (name, description, sample preparation, procedure, results):</p> <p>50-cm long pellet column heated at the bottom (140°C) and hydrated on top with Pearson water since 2012. Online measurement of water intake, axial pressure, temperature and relative humidity. Dismantling and physical determinations performed in November 2021 (water content, dry density, MIP). Mineralogical and geochemical characterisation of the material were performed (described in Deliverable 7.7).</p> |
| <p>2.1.2.5 Schedule and expected date(s) of results delivery:</p> <p>Dismantling and basic final characterisation in 2021, results delivered at the end of 2021 and report in 2022. The analyses described in Task 3.1 were performed and delivered in 2022.</p> |

Table 2-2. CIEMAT – Medium-scale lab TH cell (Bara-Kade)

| | |
|----------|--|
| 2.1.2.6 | Material (BoM item): Bara-Kade bentonite |
| 2.1.2.7 | Material treatment (sample preparation for test and loading procedure): The as-received material ($w=8.2\%$) was mixed with deionised water to reach a water content of 17%. After stabilisation for 9 days, the clay was uniaxially, statically compacted in five layers inside the cell to reach an overall dry density $\sim 1.55 \text{ g/cm}^3$ |
| 2.1.2.8 | Temperature (to which material was/will be exposed to) and exposure time Heater $T=150^\circ\text{C}$ and temperatures on the opposite side $\sim 50^\circ\text{C}$. Exposure time: ~ 3 years |
| 2.1.2.9 | Tests carried out (name, description, sample preparation, procedure, results): Two 10x10 cm bentonite columns heated at the bottom (150°C) and hydrated on top with glacial and saline water for ~ 3 years. Measurement of water intake, radial pressure, temperature and relative humidity. Heating started in January 2021 and hydration in May 2021. Dismantling and physical determinations (water content, dry density, MIP) took place in September 2023 for one of the cells and in January 2024 for the other one. |
| 2.1.2.10 | Schedule and expected date(s) of results delivery: Mounted in 2021. Dismantled in 2023-2024. Dismantling report issued in February 2024. |

Table 2-3. CIEMAT – Medium-scale lab cell: infiltration at high T

| | |
|----------|---|
| 2.1.2.11 | Material (BoM item): FEBEX granulate |
| 2.1.2.12 | Material treatment (sample preparation for test): Samples compacted directly into hermetic cell at high density (1.6 g/cm^3) with hygroscopic water content (13-14%) |
| 2.1.2.13 | Temperature (at which measurement/test is carried out) 20-140°C |
| 2.1.2.14 | Tests carried out (name, description, sample preparation, procedure, results): 10x10 cm cell with online measurement of radial and axial mechanical pressure and water intake. Infiltration with deionised water under isothermal conditions. The overall temperature of the bentonite during the tests was kept constant. The tests were kept running for ~ 3 years and after dismantling the physical state of the bentonite was characterised (dry density, water content, MIP). |
| 2.1.2.15 | Schedule and expected date(s) of results delivery: Tests started in 2020. Data delivered in 2023-2024 |

2.2 Procedures

2.2.1 Large-scale lab TH cell (HEE-B)

With the aim of simulating in the laboratory the conditions in one of the barrier materials used in the HE-E in situ test, a 50-cm long column of a granulate of MX-80 bentonite pellets was heated on its base at 140°C while Pearson water was supplied through its upper surface at a very low pressure (cell HEE-B). The test were carried out in a Teflon cell equipped with relative humidity and temperature sensors (*Figure 2-1*) and started in the framework of the UE PEBS project. The test consisted of a heating phase that lasted from November 2011 to June 2012 (with the heater temperature set initially at 100°C and finally at 140°C) and a heating+hydration phase that went on for more than 9 years. A detailed description of the experimental setup and methodology can be found in [6].

The cell dismantling was accomplished in November 2021. The heater was switched off, the sensors were removed, the bentonite column was extracted from the cell and weighed, measured and subsampled in horizontal slices as shown in *Figure 2-2*. The dismantling and subsampling operations are described in detail in [7].

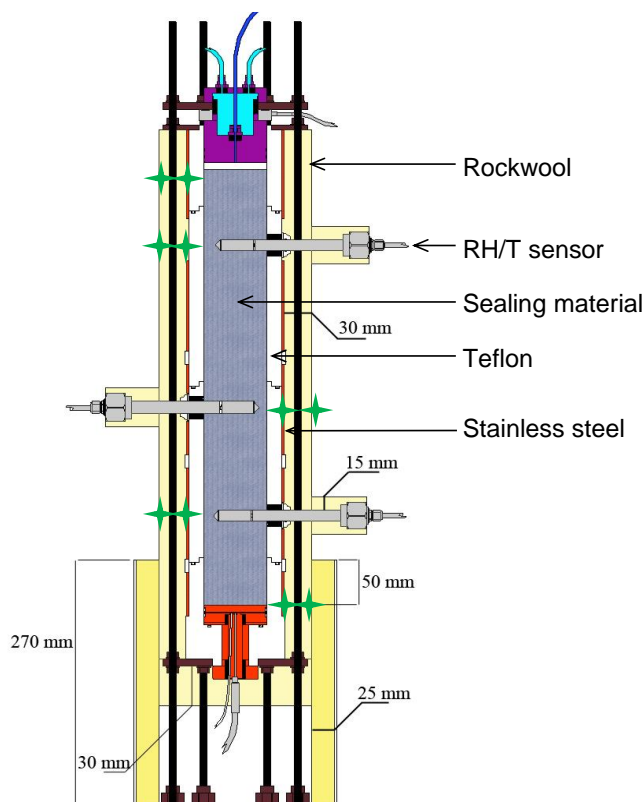


Figure 2-1. Schematic design of cell HEE-B and sensors with the external insulation (green crosses are temperature external sensor positions)

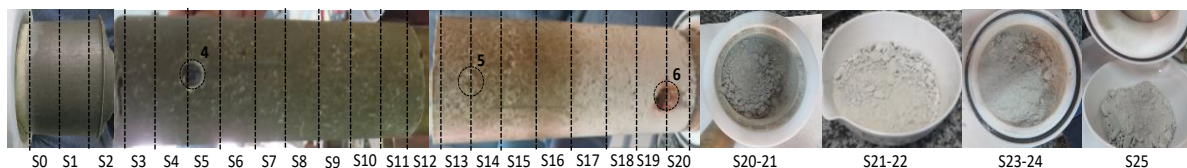


Figure 2-2. Appearance of the 26 sampling sections of the bentonite column of test HEE-B (hydration zone on the left, the photographs may show deformed diameters along the column which are not real)

2.2.2 Medium-scale lab TH cells

Two new tests, HT1 and HT2, were mounted in stainless steel cells previously used in research financed by Posiva and carried out in collaboration with Amphos 21 ([8]). The internal dimensions of the cells are 10x10 cm, and they were instrumented with four capacitive sensors (measuring relative humidity and temperature) placed at three different levels inside the bentonite and three radial stress sensors placed at the bentonite/cell contact (*Figure 2-3*). The temperatures on the cells' surface were measured with thermocouples. At the bottom of the cells a stainless-steel heater was placed. The upper part of the cell includes a cooling chamber where a cooling fluid was circulated through at a temperature of 20°C. Hydration took place through a stainless-steel porous plate placed on top of the sample. The hydration solution came from a pressurised flask located 1 m above the cells. The weight of the flask was continuously measured, which allowed the assessment of cell water intake.

Bara-Kade bentonite with a water content of 17% (reached by the addition of deionised water) was compacted inside the cells in five layers at a dry density of 1.55 g/cm³. The sensors were inserted, and the cells were wrapped in isolating material (*Figure 2-4*). After two months the cooling system was switched on and the temperature of the heater was increased from room to 150°C in 9 days. After three months, hydration started with glacial water for cell HT1 and with saline water for cell HT2. The glacial water was very dilute (TDS=6 mg/L) and the saline water contained sodium, calcium and chloride with a TDS of ~10000 mg/L.

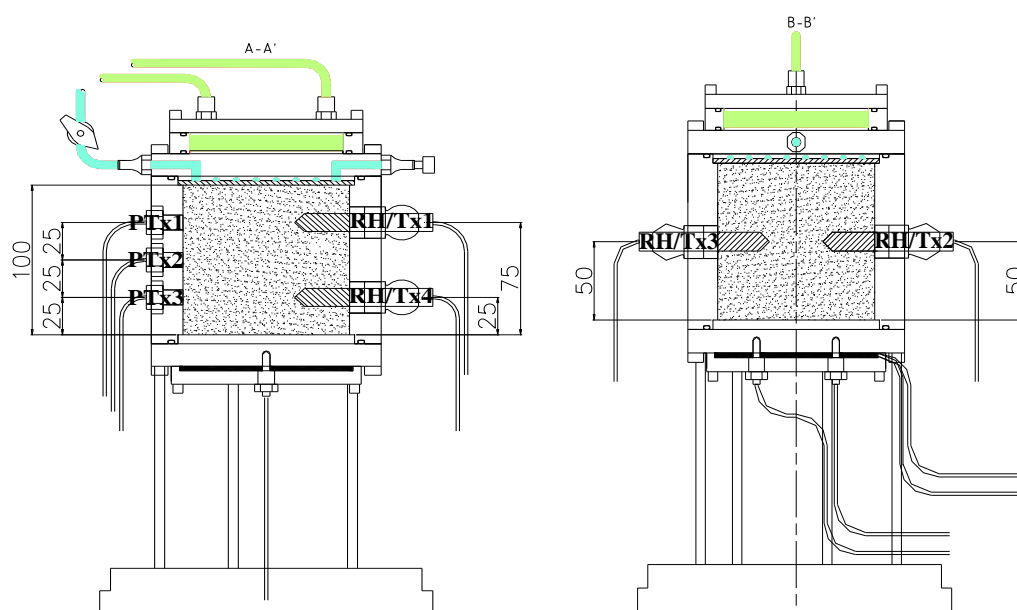


Figure 2-3. Longitudinal cross-sections of the HT cells with the sensors installed (in the sensors name, x stands for the cell number, 1 or 2)

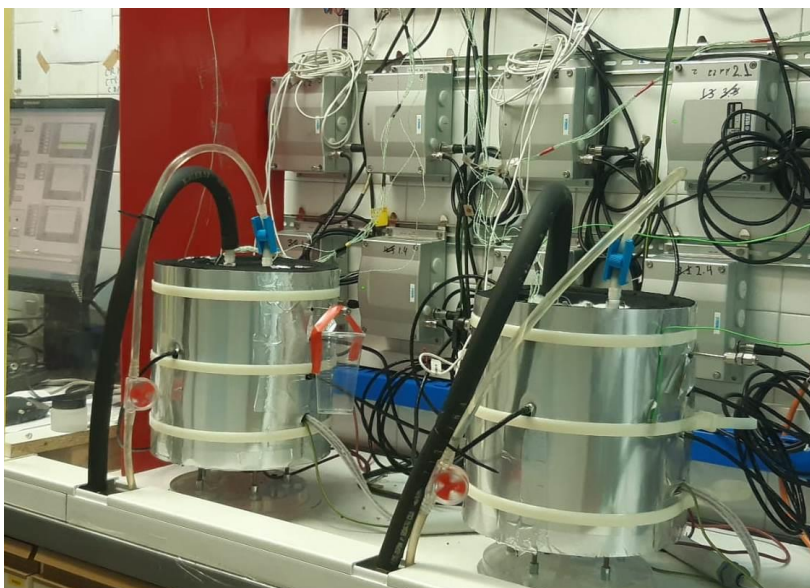


Figure 2-4. HT-1 and HT-2 cells wrapped with isolating material during operation

2.2.3 Medium-scale lab cell: infiltration at high T

A stainless-steel cell able to work at high temperature was designed and manufactured. The cell has an inner diameter of 100 mm and the same inner height (*Figure 2-5*). It is set in a rigid frame that hinders the displacement of the upper lid, which is in contact with a load cell (placed in the upper bar of the frame) to measure axial stress. Three pressure sensors are inserted at different heights through the cell wall. The cell is wrapped with a silicone heatingmat and isolated with wool rock (*Figure 2-6*). All the sensors as well as the heating system were calibrated prior to testing. Deionised, degassed water was injected with a GDS pressure/volume controller through a porous plate placed at the bottom of the cell.

The bentonite was compacted with hygroscopic water content inside the cell at a dry density of 1.6 g/cm³. Most tests started by a heating phase during which the temperatures were increased at 20°C intervals up to 150°C, waiting for the sensor stabilisation before a new temperature increase. Afterwards hydration started. The characteristics of the tests performed are shown in Table 2-4. Tests ET_1 to ET_5 were trial tests to fine-tune the cell and procedures. After the first two tests, the cell body had to be remade in certified AISI 316 stainless-steel because of the internal pitting corrosion.

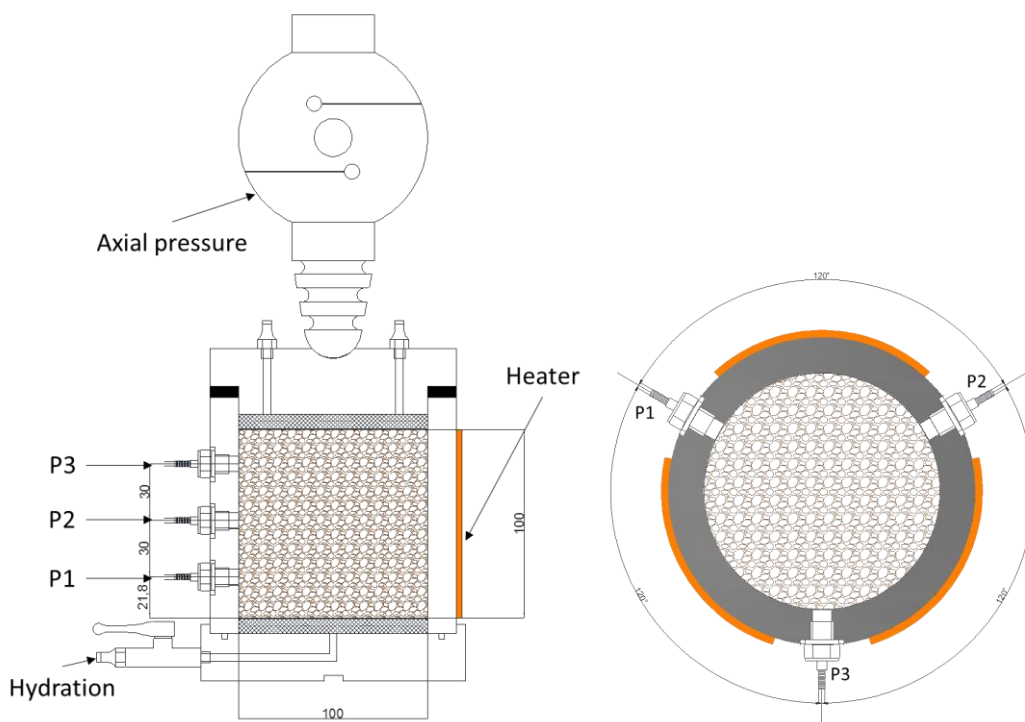


Figure 2-5. Schematic design of the high-temperature oedometer (vertical and horizontal cross-sections)



Figure 2-6. Isothermal cell wrapped in the heating mat and isolating material (left) and placed in the frame with load cell on top (right)

Table 2-4. Characteristics of the tests performed in the high-temperature oedometer (ET_1 to ET5 were trial tests, ET_8 failed)

| Reference | Compaction layers | Initial ρ_d (g/cm ³) | Initial w (%) | Maximum T (°C) | Hydration P (MPa) | Heating (days) | Hydration (days) | Final ρ_d (g/cm ³) | Final w (%) |
|-----------|-------------------|---------------------------------------|-----------------|------------------|---------------------|----------------|------------------|-------------------------------------|---------------|
| ET_1 | 2 | 1.50 | 13.3 | 150 | - | 25 | 0 | 1.51 | 7.3 |
| ET_2 | 2 | 1.50 | 7.3 | 150 | 0.015 | 8 | 37+8 | 1.41 | 27.6 |

| Reference | Compaction layers | Initial ρ_d (g/cm ³) | Initial w (%) | Maximum T (°C) | Hydration P (MPa) | Heating (days) | Hydration (days) | Final ρ_d (g/cm ³) | Final w (%) |
|-----------|-------------------|---------------------------------------|-----------------|------------------|---------------------|----------------|------------------|-------------------------------------|---------------|
| ET_3 | 2 | 1.48 | 13.6 | 150 | 1 – 0.015 | 27 | 10+27 | 1.45 | 20.4 |
| ET_4 | 2 | 1.50 | 14 | 150 | 1 | 83 | 62 | 1.44 | 26.8 |
| ET_5 | 5 | 1.60 | 13.7 | 150 | ramp | 164 | 133 | 1.66 | 5.2 |
| ET_6 | 5 | 1.58 | 14.3 | 120 | 0.6 | 126 | 124 | 1.54 | 27.0 |
| ET_7 | 5 | 1.60 | 14.6 | 140 | 0.6 | 133 | 132 | 1.54 | 25.6 |
| ET_8 | 5 | 1.58 | 14.6 | 150 | 0.6 | 17 | 16 | 1.58 | 18.1 |
| ET_9 | 5 | 1.60 | 13.2 | Room T | 0.6 | - | > 155 | ongoing | ongoing |

2.3 Results

The TH experiment with MX-80 pellets and heater at 140°C started in 2012 and was dismantled in November 2021 after 10 years of operation. Two new TH cells were mounted using Bara-Kade bentonite and started heating at 150°C in January 2021. Hydration with glacial and saline water started in May 2021 and the cell hydrated with saline water was dismantled in September 2023. A cell to perform infiltration tests at high temperature with measurement of axial and radial pressures was designed, tested and upgraded and isothermal tests with FEBEX bentonite took place at temperatures of 120°C and 140°C. The results of each of these tests are described below.

2.3.1 Large-scale lab TH cell (HE-E)

The initial results of this cell were reported in [6] and the final report with the whole series of online results and the final physical state of the bentonite can be found in [8]. The heating phase showed that the thermal conductivity of the dry materials is low, which caused a high difference in temperature between the heater surface and the sensor located at 10 cm, generating a high thermal gradient near the heater, and low temperatures in the rest of the column. In fact, the initial thermal conductivity of the material was lower than that of Teflon (0.12 vs. 0.25 W/mK), and the heat transmission could have taken place during the initial phases of the experiment preferentially along the Teflon wall. The stabilisation of the temperature was very quick. The power needed to keep a temperature of 100°C at the heater surface was 8 W and for a temperature of 140°C was 12 W. The steady-state temperatures were probably affected by the presence of the steel reinforcement on the Teflon surface and by the good thermal contact between the heater plate and the pellets, because of the well-sorted grain size distribution of the pellets, which allows for the filling of pores (*Figure 2-7*). On the other hand, heat conduction and dissipation through the bottom of the cell could have taken place despite the insulation material, and this could be the reason why the temperatures inside the pellets were not as high as expected, specially taking into account the high power supplied by the heater ([9]).

The movement of water in the vapour phase because of the thermal gradient was evinced by the increase in relative humidity recorded by the sensor closest to the heater –followed by a continuous decrease– and the slower increase recorded by the two other sensors (see *Figure 2-1* for location of sensors). At the end of the heating phase the relative humidity gradient was not very sharp, which made that before hydration, the highest relative humidity was recorded in the middle of the column (*Figure 2-7*).

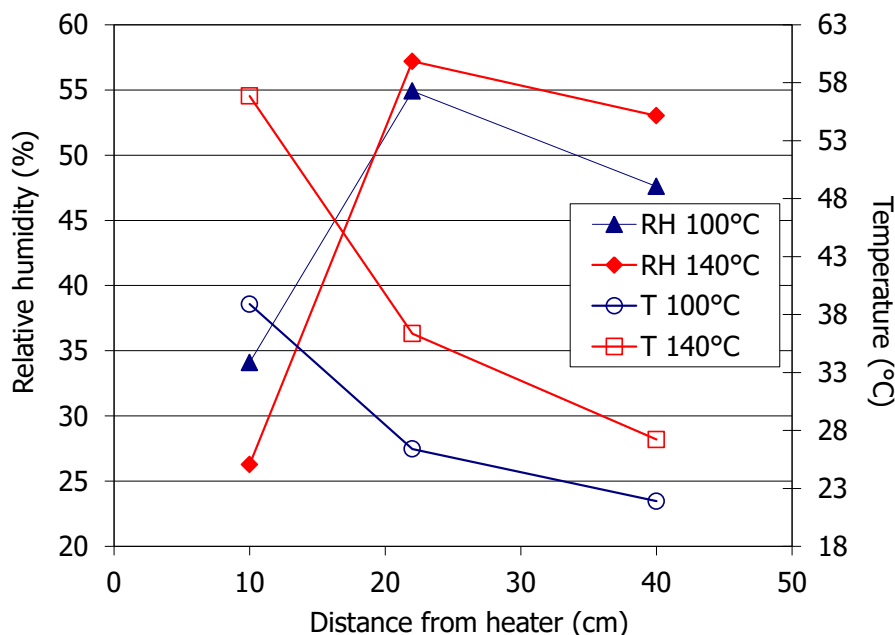


Figure 2-7. Equilibrium values measured inside the material after the heater was set to 100°C ($t=3524$ h) and 140°C ($t=5015$ h) in cell HEE-B

During the hydration phase the temperatures remained approximately constant, with a slight seasonal laboratory temperature oscillation. The average temperatures during the hydration phase are plotted in Figure 2-8 as a function of the distance from the heater. A steep thermal gradient is observed in the 10 cm closest to the heater. The temperatures measured on the surface of the cell with thermocouples set on the steel semi-cylindrical pieces and outside the cell (at the locations indicated by green stars in Figure 2-1) are also plotted in the Figure. The temperatures inside the bentonite were mostly conditioned by the distance from the heater but not by the distance to the cell axis (except close to the heater), which indicates that the temperature distribution followed a uniaxial pattern.

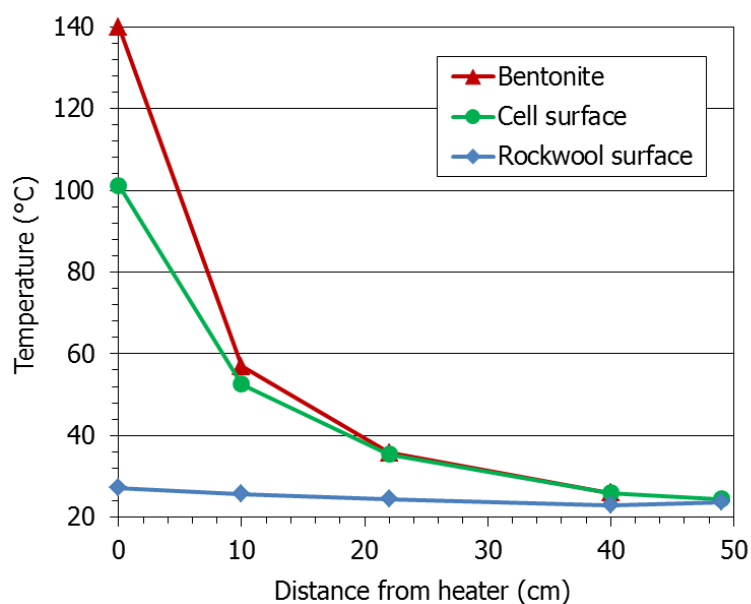


Figure 2-8. Average temperatures along the column measured by the sensors inside the cell and external temperatures measured with thermocouples from June 2013 to June 2021

The low water permeability of the pellets was highlighted by the fact that after more than 300 h of hydration, the upper sensor had not yet recorded any RH change and that it took more than 5 years of hydration for the relative humidity at the location of sensor 3 (40 cm from the hydration surface) to reach the initial 40% value. However, sensor 2, placed at the middle of the column, became flooded after 1863 days of hydration, which would indicate that the liquid water front had reached this part of the column. In contrast, the decrease in RH recorded by the upper sensor could be related to the decrease in the degree of saturation caused by the dry density decrease (*Figure 2-9*). Sensor RH3 failed shortly before dismantling.

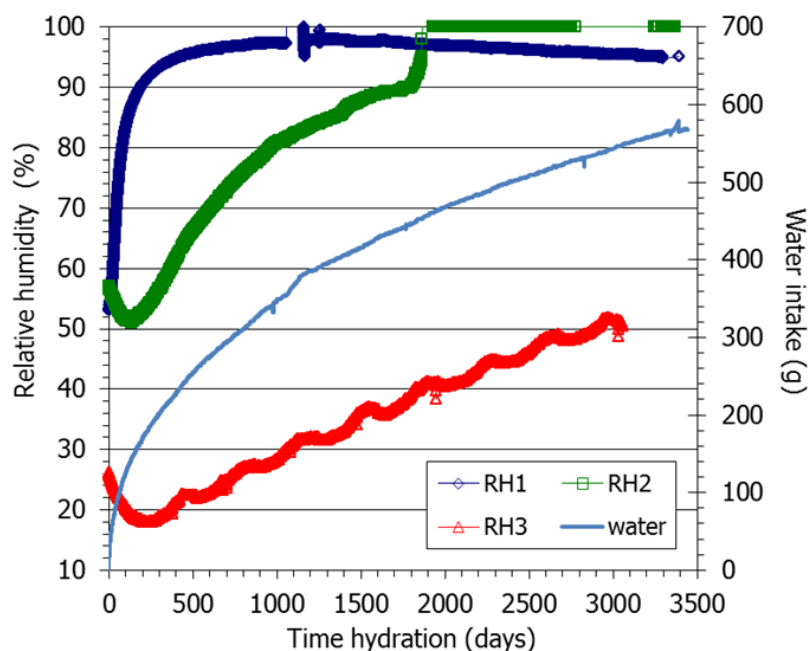


Figure 2-9. Evolution of water intake and relative humidity in cell HEE-B after the beginning of hydration (sensor 1 placed at 40 cm from the heater, sensor 2 at 22 cm and sensor 3 at 10 cm)

Upon dismantling it was seen that the upper half of the column had water contents around 30%, which only increased above this value in the 5 cm closest to the hydration surface (*Figure 2-10*). These high water contents correspond to uniform degrees of saturation between 92 and 99% in the upper half of the column, where the bentonite was compact and dark, with a smooth appearance in which no pellets could be told apart. In contrast, the water content and degree of saturation sharply decreased towards the heater in the bottom half of the column, with values close to 0% in the 5 cm closest to the heater. At less than 16 cm from the heater the bentonite was lighter in colour and was loose. In this respect, the dry density of the upper 30 cm was lower than the initial one (particularly close to the hydration surface) but tended to increase towards the heater, where it was difficult to determine because of the disaggregated state of the granulate. The bentonite in the more saturated part of the column would be expanding downwards, towards the drier and more compressible bentonite. This process would give place to the observed dry density gradient, reported in many previous investigations. The best estimation of the average final water content of the column is 22.0%, and of the dry density 1.52 g/cm³, corresponding to a degree of saturation of ~75%.

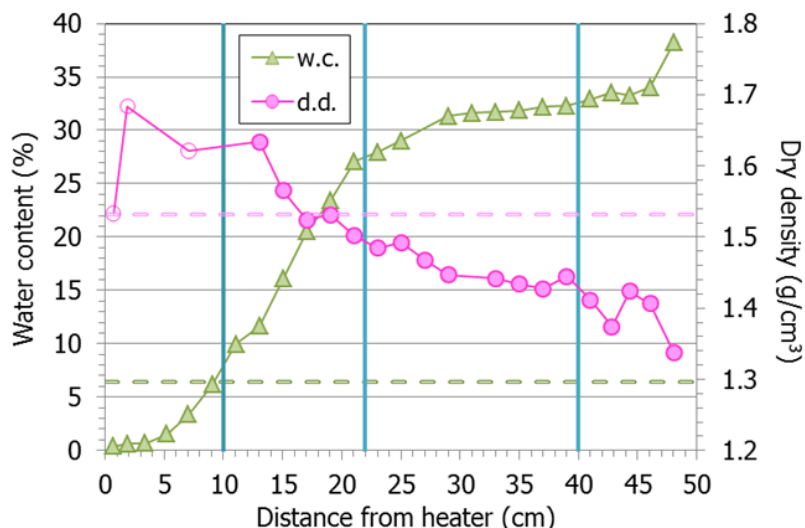


Figure 2-10 Water content and dry density of the column measured at the end of the test HEE-B (empty symbols: estimated from weight and volume). The thick vertical lines indicate the location of sensors, and the dotted horizontal lines the initial values

The discrepancy between the actual water intake determined upon dismantling and the online measurements (Figure 2-9 which overestimated the water intake in ~20%) points to vapour leaking taking place during operation, possibly via the sensors' orifices, particularly the bottom one located at 10 cm from the heater. In fact several physical, mineralogical and geochemical particularities were detected in this area during the postmortem analysis of the bentonite ([10]).

The axial pressure measured during operation on top of the cell was mainly linked to the RH increase in the bentonite upper 10 cm (Figure 2-11). For this reason, this pressure reached a value of 1.4 MPa after 300 days of hydration and increased very slowly afterwards, keeping at the end of the test in values between 1.4 and 1.6 MPa, which would correspond to the saturated swelling pressure of the MX-80 bentonite compacted to a dry density of ~1.35 g/cm³. This is the average density measured in the upper centimetres of the column, which would evince that the load cell on top of the cell measured a local value. Given the Teflon cell surface, friction was probably not relevant during the test and in fact the saturated parts of the bentonite column were extracted from the cell applying without applying significant pressure.

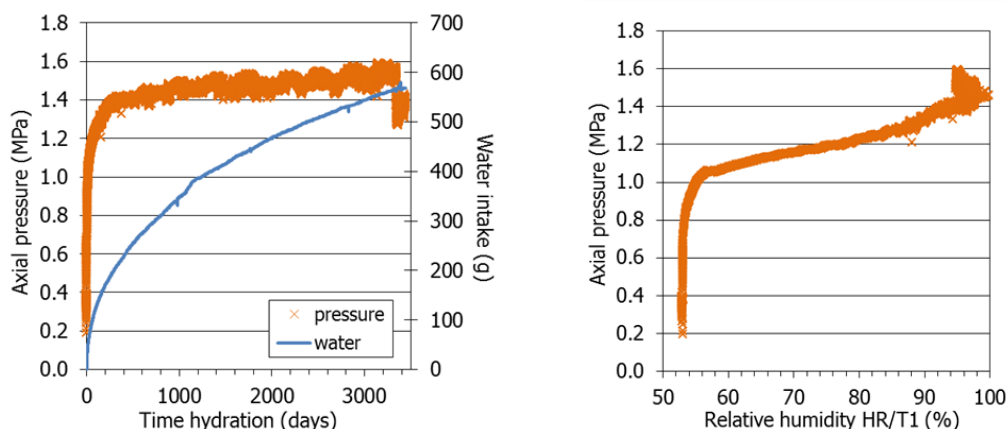


Figure 2-11 Axial pressure measured on top of cell HEE-B and water intake from the beginning of hydration (left) and relation between relative humidity measured by sensor 1 and axial pressure (right)

2.3.2 Medium-scale lab TH cells

Two new tests, HT1 and HT2, were mounted in cylindrical stainless-steel cells of dimensions 10x10 cm. The initial conditions of the Bara-Kade bentonite were the same for the two tests ($\rho_d=1.55 \text{ g/cm}^3$, $w=17\%$), and the heating phase was similar in the two tests: the heater temperature was increased from room to 150°C in 9 days, and it remained in this value for 3 months. Then, hydration started with glacial water for cell HT1 and with saline water for cell HT2. The heaters' power to keep the target temperature was 10 W.

The evolution of temperature and relative humidity inside the bentonite during the heating phase is shown in *Figure 2-12* and the steady values reached at the end of it are shown in *Figure 2-13*. Thermal equilibrium was quickly reached, and the thermal gradient measured inside the bentonite and on the external surface of the cell was similar. The water vapour moved towards the upper part of the cell, where the relative humidity started to increase first at the bottom sensor location and then in locations upwards. After less than 10 days the bottom of the samples started to dry out (sharp decrease in relative humidity) and some days later the middle part of the samples also experienced a decrease in relative humidity, evincing the upwards vapour movement. In the two cells the upper radial pressure sensor recorded an increase up to 2 MPa after 20 days of heating and then a slow decrease. At the end of the heating phase none of the pressure sensors recorded positive values.

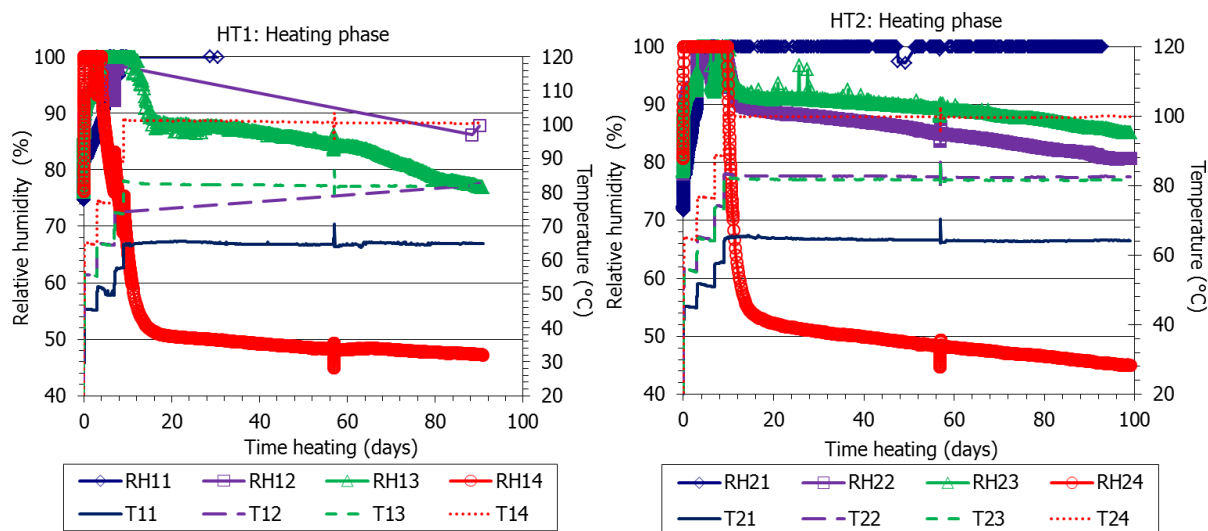


Figure 2-12. Time evolution of relative humidity and temperature inside the bentonite during the heating phase of tests HT1 and HT2

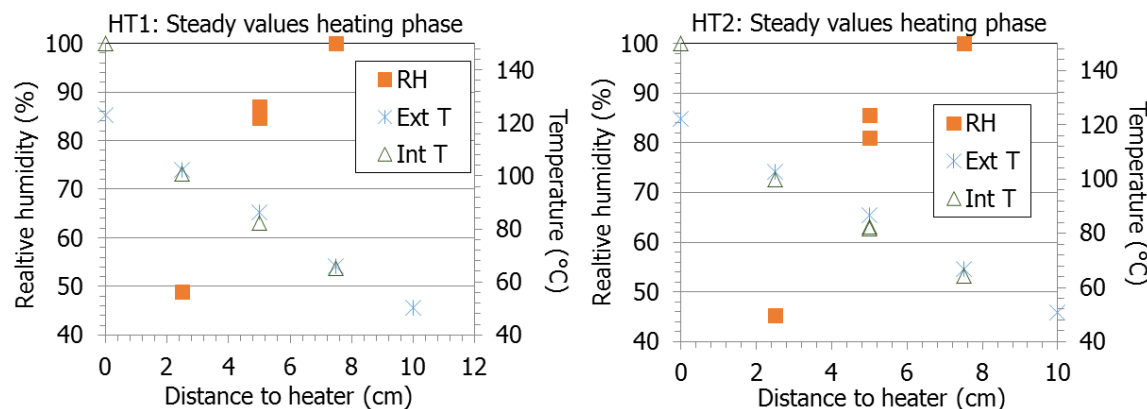


Figure 2-13. Temperatures and relative humidity inside the bentonite at the end of the heating phase of tests HT1 and HT2

After the three initial months of heating, leading to quasi-steady hydraulic conditions, hydration started in May 2021. During hydration, the temperatures remained constant and in the same values as before, as shown by the external temperature sensors. The relative humidity measured by the middle sensors in the two cells went to 100% in a few days, which indicates their flooding or vapour condensation. Only the RH sensors at the bottom part (at 2.5 cm from the heater) recorded a steady increase for ~90 days. At this time a supervised overheating episode (described below) altered the behaviour of the system and the RH/T sensors failed, including the temperature measurement. The radial pressure sensors in the upper and middle parts of the cells had recorded increasing trends since the beginning of hydration (quicker in the upper sensors), while the bottom sensors did not record any changes (*Figure 2-14, Figure 2-15*). The pressure values at the same location were higher for cell HT1, hydrated with glacial water, which is consistent with the salinity-induced reduction of swelling capacity.

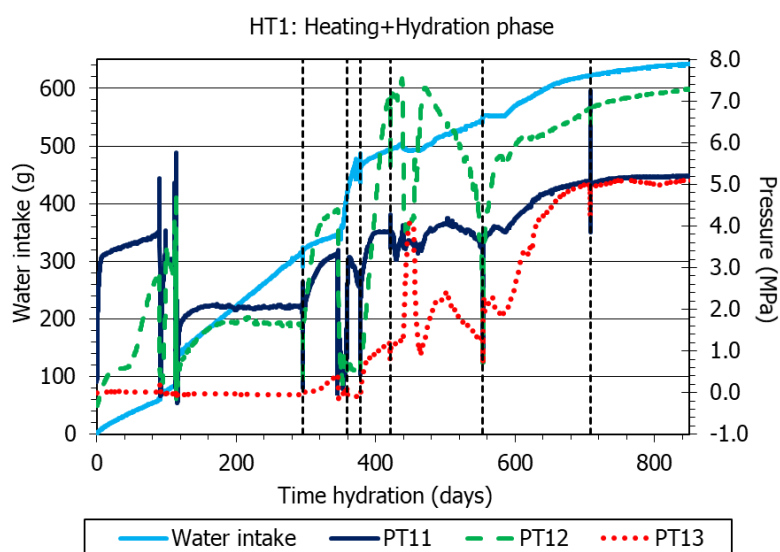


Figure 2-14. Evolution of radial pressure during hydration with glacial water of cell HT1 (PT13 at 2.5 cm from the heater, PT12 at 5 cm and PT11 at 7.5 cm)

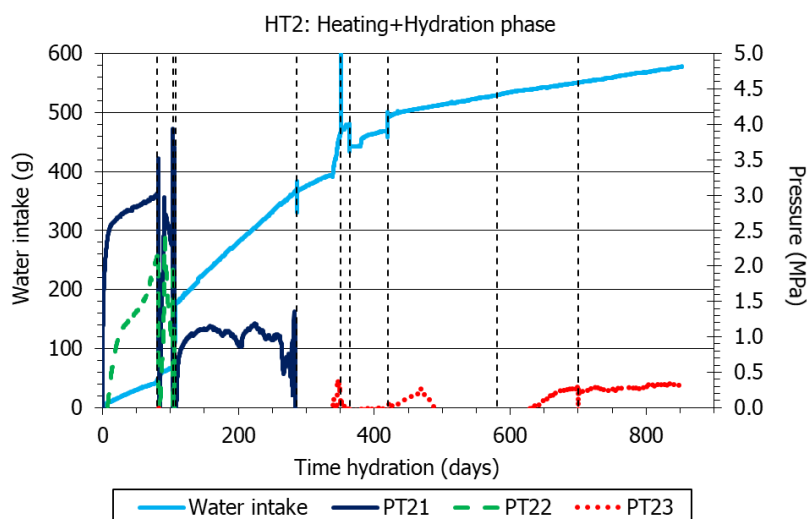


Figure 2-15. Evolution of radial pressure during hydration with saline water of cell HT2 (PT23 at 2.5 cm from the heater, PT22 at 5 cm and PT21 at 7.5 cm)

As a result of an air conditioning failure on August 8th 2021 (after 80 days of hydration), concurrent with a heat wave in Madrid, the temperature in the laboratory reached values of 42°C. The chiller system on

top of cells HT1 and HT2 failed and the temperatures reached 106°C in the bentonite upper part. For some days the chiller in charge of cooling the upper part of the cells kept going on and off and the temperatures experienced abrupt changes (between days 80 and 130), resulting in the failure of the RH/T sensors and sudden changes in radial pressures. These features can be seen in the Figures above. Afterwards, once the chiller was replaced and the temperatures had come back to normal, an increased water uptake rate was observed, as well as a persistent drop in the radial pressure measured between the bentonite and the cell wall. This behaviour was attributed to some water leak resulting from alternating thermal expansion and contraction of the cell elements and/or deterioration of some of them because of the excessive temperatures. The leaks possibly took place through the sensors' openings. Hence, it was decided to reseal these openings. For that, approximately at day 300, the heater and cooling systems were switched off, the hydration inlet was closed and the insulating material around the cell was removed. The RH sensors' inlets (in some of which water drops could be observed) were sealed with silicone at all possible places. The operation of the cells resumed and an improvement in their behaviour was observed since then, with a reduction in the water intake rate in both cells and an increase of the radial pressure in cell HT1. However, no proper measurement of the radial pressure sensors of cell HT2 was achieved. Several power outages took place during operation what caused cooling/heating episodes that are marked by vertical discontinuous lines in *Figure 2-14* and *Figure 2-15*. It became clear that, despite the resealing performed, the inlets of the RH/T sensors were leak pathways and some of them were even expelled out of the cell, causing a sudden increase in the water intake rate (RH/T1.1 and 1.4). Hence it was decided to remove them (since they were not providing any information) and closed the inlets with bolts. Sensors RH/T1.1 and 1.4 (cell HT1) were removed after 378 days of hydration and sensor RH/T1.2 after 554 days of hydration. All the RH/T sensors in cell HT2 were removed and their inlets closed after 420 days of hydration.

After 871 days of hydration the water intake and the radial pressures in cell HT1 seem to have stabilised. The pressures measured by the upper and lower sensors are ~5 MPa and by the middle sensor higher than 7 MPa.

Cell HT2 was dismantled after 852 days of hydration. The middle and bottom radial pressure sensors had started to record a soft increase after 600 days of hydration, but to values only slightly above 0 MPa. The offset of the pressure sensors was probably altered as a result of all the sudden temperature changes and the absolute values measured are not reliable.

Upon extraction the upper part of the bentonite block was consistent, dark and wet. The bottom part was completely disaggregated (*Figure 2-16*). Overall, the bentonite presented numerous stain marks, particularly around the sensors' filters. The final weighing of the bentonite allowed to check that the actual water intake had been <90 g, whereas the online system gave a value >500 g. This difference attests the continuous water evaporation that took place through the sensor inlets until they were sealed.



Figure 2-16. Upper part of the block from cell HT2 and material corresponding to the section closest to the heater

The consistent part of the block was cut into 2-cm thick sections with a saw. The sections were numbered from 1 (uppermost) to 5 (closest to the heater). Because the bentonite block was damaged at the bottom, sections 4 and 5 could not be clearly defined. In subsamples of these sections water content and dry density were determined. To determine the water content the samples were dried in the oven at 110°C for 48 h. To determine the dry density the volume of the samples was determined by immersing them in a recipient containing mercury and by weighing the mercury displaced, considering a density of mercury of 13.6 g/cm³. Figure 2-17 shows the final water content, dry density and degree of saturation values along the bentonite block of cell HT2. There were relevant gradients between top and bottom of the block both in terms of water content and of dry density. The upper part of the block had degrees of saturation higher than 90%, but the 4 cm closest to the heater had water content and degree of saturation below the initial ones.

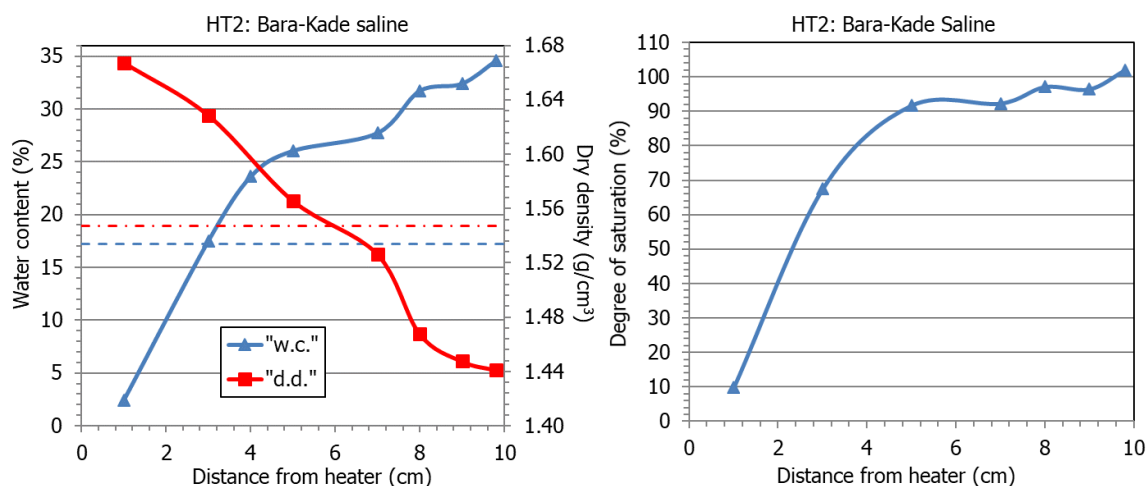


Figure 2-17. Final water content (w.c), dry density (d.d.) and degree of saturation along the bentonite block of cell HT2 (~2.5 years of hydration with saline water under a high thermal gradient). The discontinuous horizontal lines indicate the initial values

2.3.3 Medium-scale lab cells: infiltration at high T

Two isothermal tests at 120 and 140°C (tests ET6 and ET7) were performed. Hydration with deionised water started only two days after the beginning of heating. In the two cases the radial pressures measured increased progressively with hydration time. In contrast, the axial pressure increased initially

more than the radial ones and then softly decreased until reaching a stable value. The final degree of saturation was close to 100% in the two cases. *Figure 2-19* shows the final radial and axial pressure values for the two tests. The swelling pressure at room temperature corresponding to a FEBEX bentonite sample of dry density 1.6 g/cm³ would be ~6 MPa. Hence, the values measured are lower than expected, especially for the higher temperature. Indeed, the decrease of swelling pressure with temperature for the FEBEX bentonite has been previously demonstrated ([11]).

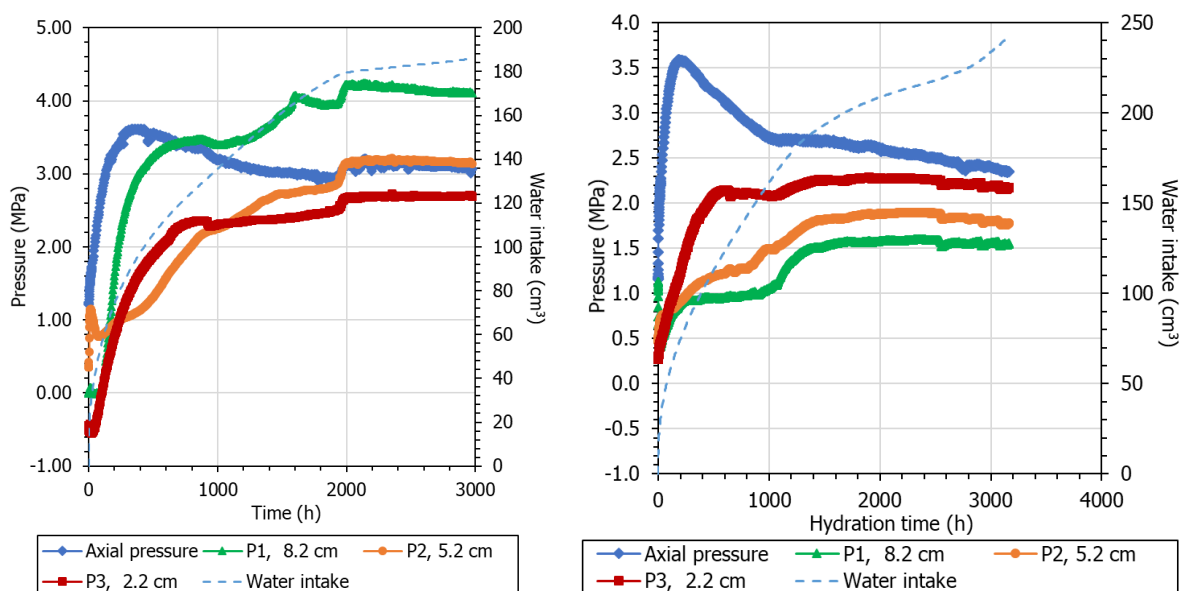


Figure 2-18. Pressure and water intake evolution in test ET6, isothermal at 120°C (left) and test ET7, isothermal at 140°C (right). The distance to the hydration surface of the radial pressure sensors P1, P2 and P3 is indicated in the legends.

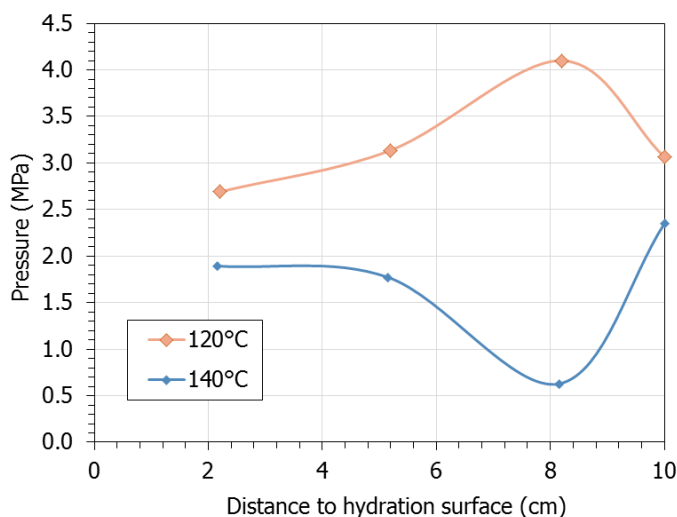


Figure 2-19. Radial and axial (at distance 10 cm) pressures measured in two hydration tests performed under isothermal conditions (FEBEX bentonite compacted at 1.6 g/cm³ saturated with deionised water)

Figure 2-20 shows the final distribution of water content and dry density along the two bentonite blocks. The figure shows average values of determinations performed in the internal and external parts of the blocks, which presented some differences (not shown), indicating possible wall effects. Additionally, the water contents tended to be higher towards the ends of the blocks, particularly the top one, which also had the lowest dry density. This effect could be related to the vapour movement by gravity towards the upper part of the blocks and is more intense in the test at higher temperature.

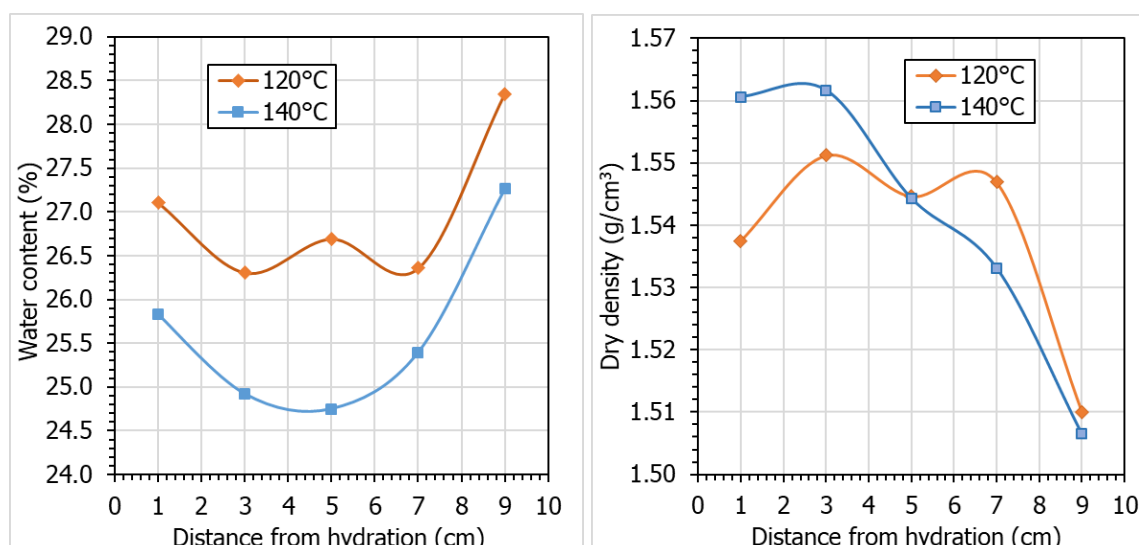


Figure 2-20. Final distribution of water content and dry density in two hydration tests performed under isothermal conditions (FEBEX bentonite compacted at 1.6 g/cm^3 saturated with deionised water)

2.4 Conclusion

Three thermo-hydraulic tests in which the heaters were set at temperatures of 140 and 150°C have been carried out, one of them was dismantled after 10 years of operation (test HEE-B), another one after 2.5 years of hydration (tests HT2) and the other one is still running. Experimental artefacts, namely evaporation through the sensors' inlets, hindered the saturation of the bentonite closest to the heater, which remained very dry in cells HEE-B and HT2. However, relevant radial swelling stresses – associated to the increase in water content– were recorded during saturation, higher when diluted water was used instead of saline one. The infiltration tests performed under isothermal conditions ($T=120^\circ\text{C}$ and 140°C) showed relevant pressure build up, although with values lower than expected for room temperature.

The hermeticity of the cells seems to be determinant for the behaviour observed. If vapour is unable to escape, as seems to be the case in cell HT1, very high swelling pressures can be developed, even when the heater temperature is 150°C .

At the end of the tests, significant gradients in the water content and dry density distributions had been developed in the bentonite, with higher water contents close to the hydration surface, where the dry density was lower. However, in the isothermal tests, where hydration took place through the bottom of the samples, the dry density distribution followed the opposite trend, with the lower values measured on the block side opposite to the hydration surface, where also the highest water contents were measured. This distribution likely results from the upwards vapour movement.

The results of test HEE-B have been used to validate the model developed by UPC and described in D7.10 and as a benchmark in the DONUTS project.

3. CTU (SÚRAO)

3.1 Introduction

The purpose of the experiments carried out was to obtain the characteristics of bentonite after exposure to high temperature (up to 150 °C) with forced saturation (3,5 - 6 bar) and to test its behaviour on a medium scale. The data obtained in the benchmark experiment were intended to be used in the mathematical modelling part of Subtask 3.3. The aim of the benchmark was to gather information necessary to simulate the THM processes occurring in the bentonite under overall constant volume conditions, while both thermal loading and forced saturation pressure were active. Another purpose was to verify the measurements from Subtask T3.1 on a larger scale.

As part of subtask T3.3, two experiments were performed. After the dismantling of each experiment, samples were taken and analysed as part of the laboratory work in subtask T3.1. The water content field and dry density at different locations inside the bentonite block were determined. The hydraulic conductivity, swelling pressure and liquid limit determined on samples taken from different locations in the experiment were also analysed.

3.1.1 Material

Czech origin bentonites are considered to be used as buffer and backfill material in the Czech deep geological repository, thus the research in HITEC project has focused on Czech bentonite of calcium/magnesium (Ca/Mg) type extracted from the Černý Vrch deposit. The material had been extracted and processed (dried and milled) by the manufacturer and the texture of final original material ready for testing is a very fine powder. The material was first subjected to testing in 2017 and its designation is BCV_2017. The basic characteristics of tested bentonite have been summarized in [12]. The data concerning the original material were acquired from other projects [12], [13], [14]. The same bentonite is used in HITEC T3.1 and T3.2.

3.1.2 Research plan

Table 3-1. CTU – Medium-scale laboratory tests

| |
|---|
| <p>3.1.2.1 Material (BoM item): BCV bentonite (Ca-Mg type), powder (first test) and pellets (second test) as delivered by producer</p> |
| <p>3.1.2.2 Material treatment (sample preparation for test):</p> <ol style="list-style-type: none"> 1) Loose powder bentonite gentle manual compaction to 949 kg/m³ 2) Manually compacted pellets to 1408 kg/m³. The dry density of the pellets was 2 g/cm³ <p>Initial water content as in delivered material (10-13%)</p> |
| <p>3.1.2.3 Temperature (at which measurement/test is carried out) 150°C at the bottom of vessel, cooling (room temperature) at the top</p> |
| <p>3.1.2.4 Tests carried out (name, description, sample preparation, procedure, results):</p> <p>Material was placed into constant volume cylindrical vessel of 300 mm diameter and 250 mm height. Temperature gradient was applied (150°C at the bottom, room temperature on top). Forced saturation was applied from the top. Two experiments were performed. The first with powdered bentonite, the second with pellets. The first test run for a year and the second one for eight months. Upon dismantling samples were analysed as part of T3.1</p> |

3.2 Procedures

The tests were carried out in a specially designed cylindrical vessel of constant volume, which allowed simultaneous thermal loading of the sample and forced saturation. Saturation was applied at the top through the lid, while a thermal load of 150°C was applied at the bottom. The sample experienced a thermal gradient from bottom to top, naturally cooled by ambient air. The monitoring system consisted of temperature sensors inside the bentonite and on the surface of the vessel, pressure sensors at the inlet, a saturation vapour pressure sensor inside the vessel and a RH meter to measure ambient humidity in the vicinity of the medium-scale laboratory experiment.

Within this subtask, two tests were carried out, each with a different type of BCV bentonite and a different dry density. The difference between the two tests was also in the experimental procedure. The first test used powdered BCV bentonite with a dry density of 949 kg/m³ and the second test used pelletised BCV bentonite with a dry density of 1408 kg/m³. In the first test, the bentonite was first saturated at room temperature and then the temperature was gradually increased to 150°C. In the second test, a procedure was chosen that was more in line with the conditions expected in a future radioactive waste repository. The second procedure consisted of simultaneous saturation and heating to the target temperature. After placing the bentonite in the vessel, heating was started directly at 150°C, followed by saturation.

Samples for laboratory analysis of hydraulic and mechanical properties were taken after dismantling of the experiment.

3.2.1 Laboratory set-up

The laboratory set-up consists of a specially designed vessel. The body of the vessel consists of a stainless-steel cylinder 300 mm in diameter and 300 mm long. Flanges are welded to both ends of the tube - top and bottom. The lid and base are blind (solid) flanges. The vessel is closed by tightening the lid to the tube flange using threaded rods with nuts, while six of the rods are tightened to the bottom flange. (*Figure 3-1*).

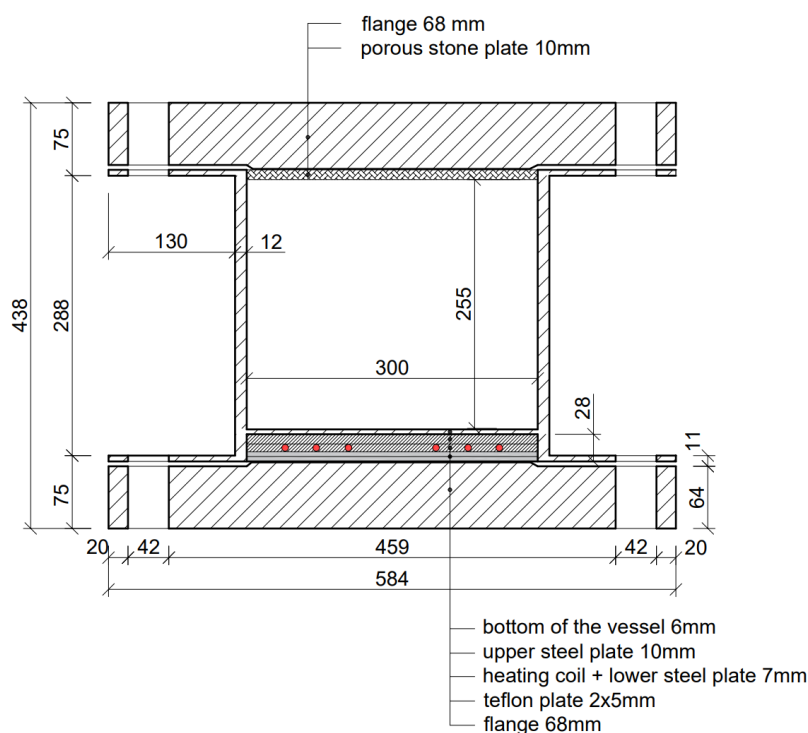


Figure 3-1. Schema of medium-scale laboratory experiment

Thermal loading was provided by a heater located in the lower part of the vessel. The heater consists of an electrical resistance coil housed in a groove in the steel plate and covered by the upper steel plate. Two Teflon plates are placed at the bottom of the heater stack as thermal insulation. The heater stack is bolted to the lower blind flange. The contents of the vessel are separated from the heater by a stainless-steel plate welded into the tube directly above the heater.

The space for the sample is limited at the sides by the tube, at the bottom by a steel plate welded to the tube above the heater, and by a 10 mm porous stone placed under the lid. The effective internal diameter is 300 mm and the effective height is 255 mm. The volume of the vessel is 0.018 m³.

Forced saturation of the bentonite is provided by a system consisting of two pressure bottles. One bottle with air serves as a pressure source, the other with distilled water as a gas-water exchanger. The required pressure is set and maintained by a regulating valve at the outlet of the air bottle. The water is fed from the gas/water exchanger into the vessel through the lid by means of an 8-mm diameter steel pipe (Figure 3 2 and Figure 3 3). Saturation took place through the opening in the centre of the lid of the vessel and uniform distribution of the water was ensured by a porous stone under the lid.

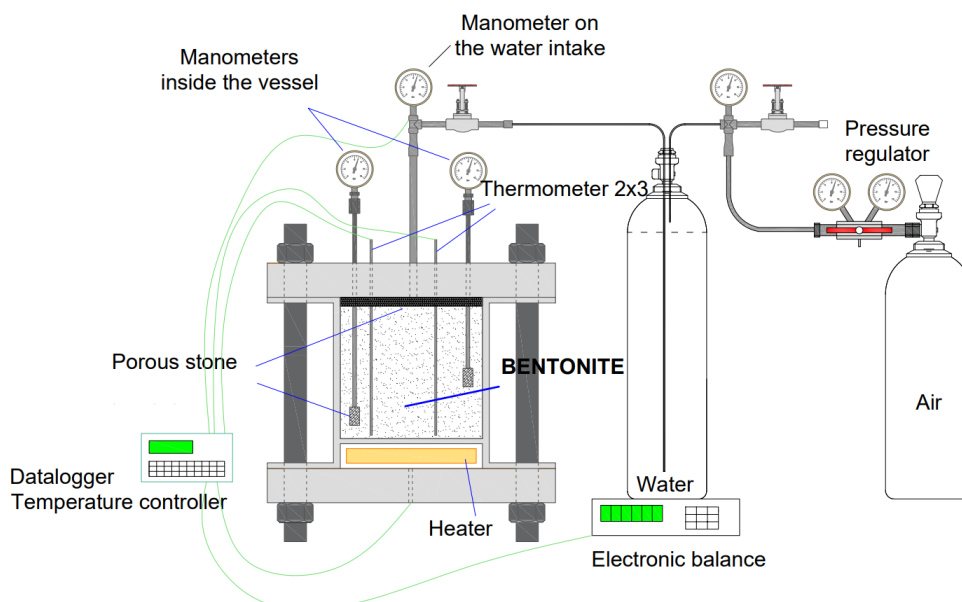


Figure 3-2. Schematic illustration of saturation system of medium-scale laboratory experiment



Figure 3-3. The experiment set-up

electronic balance. The total weight of the bentonite was 19.297 kg. Gentle manual compaction was applied. The dry density, calculated from total mass and the initial water content, was 949 kg/m³.

Pelletized Czech BCV_2017 was tested in Test 2. The aim was to test hydration of compacted pelletized bentonite. The pelletized bentonite was industrially produced, and the average dry density of the individual pellets was 2 g/cm³. The initial water content of bentonite corresponding to hygroscopic humidity at laboratory conditions was 10%. Bentonite was placed in the vessel in the same way as in the first test. The total weight of the bentonite was 27.9 kg. The bentonite was compacted by hand into the vessel using a small steel compactor. The aim was to achieve the highest possible dry density (when using manual compactor) and it was 1408 kg/m³.

The main characteristics of the samples in the first and second tests after installation are summarised in *Table 3-2*.

Table 3-2. Main characteristics of the samples in Test 1 and Test 2 after installation

| Material | BCV_2017 | |
|----------------------------------|-------------------|---------------------|
| | Powdered (Test 1) | Pelletized (Test 2) |
| Height (mm) | 255 | 255 |
| Diameter (mm) | 300 | 300 |
| Volume (m ³) | 0.018 | 0.018 |
| Weight (kg) | 19.3 | 27.9 |
| Dry density (kg/m ³) | 949 | 1408 |
| Void ratio | 65% | 48% |
| Initial water content | 13% | 10% |

Once the vessel had been filled-up by bentonite, the top porous stone plate with drilled apertures for instrumentation was placed on and the instrumentation probes were placed to their positions in the lid. Then the vessel was closed using the frame crane and a check weighing was carried out. The assembly was weighed before applying the material and afterwards. No errors in weighing were noticed.

3.2.3 Experimental procedures

Test 1

The first phase of the test was saturation at laboratory temperature. The aim was to first reach the pressure of 6 bar inside the vessel, which was necessary to achieve a non-boiling state of the liquid inside the vessel when subsequently heated to 150°C. Once the required pressure (provided by the saturation) was reached, heating began.

Hydration started on 03/12/2020. The saturation pressure was gradually increased to 6 bar, which was reached on 28/01/2021. Thermal loading started after the observed features had stabilised on 02/02/2021, keeping the saturation pressure at 6 bar. The heater was initially set at 90°C. After stabilisation of the monitored variables, the temperature was increased to 120°C and then to the final temperature of 150°C, which was the target one. The saturation pressure increased to 7.9 bar, which is more than was intended, due to manipulation of the compressed air bottle during filling. From this point the temperature of the heater was maintained at 150°C and the saturation pressure at 7.9 bar. The test was dismantled on 11.02.2022. The main stages of the first test are listed in *Table 3-3*.

Table 3-3. Key phases of Test 1

| Phase | Date | Saturation pressure (MPa) | Temperature |
|--------------------------|------------|---------------------------|-------------|
| Assembling | 03.12.2020 | 0 | 20°C |
| Start of saturation | 03.12.2020 | 0.5 | 20°C |
| Saturation pressure rise | 15.12.2020 | 3.5 | 20°C |
| Saturation pressure rise | 13.01.2021 | 4.3 | 20°C |
| Saturation pressure rise | 28.01.2021 | 6 | 20°C |
| Start of heating | 02.02.2021 | 6 | 90°C |
| Temperature rise | 12.04.2021 | 6 | 120°C |
| Temperature rise | 09.06.2021 | 7.9 | 150°C |
| Dismantling | 11.2.2022 | | |

Test 2

In the second test a different test procedure was followed. The procedure was chosen in such a way as to simulate conditions in a future repository. In the first stage of the test, the bentonite was heated directly at 150°C without saturation. Once the temperature field had stabilized, saturation with water at 3.5 bar started.

Table 3-4. Key phases of Test 2

| Phase | Date | Saturation pressure (MPa) | Temperature |
|---------------------|------------|---------------------------|-------------|
| Assembling | 14.10.2022 | 0 | 20°C |
| Start of heating | 17.10.2022 | 0 | 150°C |
| Start of saturation | 14.11.2022 | 3,5-4,6 | 150°C |
| Dismantling | 20.6.2023 | | |

3.3 Results

3.3.1 Test 1 – bentonite powder

In the first test, powdered bentonite BCV with a dry density of 950 kg/m³ was used. *Figure 3-5* shows the temperature and saturation evolution. It is possible to observe the rapid reaction of the system to the temperature increase and the rapid stabilization of the temperature inside the bentonite. The experiment was continuously saturated with distilled water through the lid. Within the first two months, 90% of the free pores were filled with water. The saturation pressure was maintained at 6 bar. The saturation vapour pressure was measured at two levels. The results show that this pressure was in equilibrium at both locations and that it increased with each increase in heater temperature. After reaching the target temperature of 150°C, the saturation vapour pressure stabilised at 8 bar within 10 days.

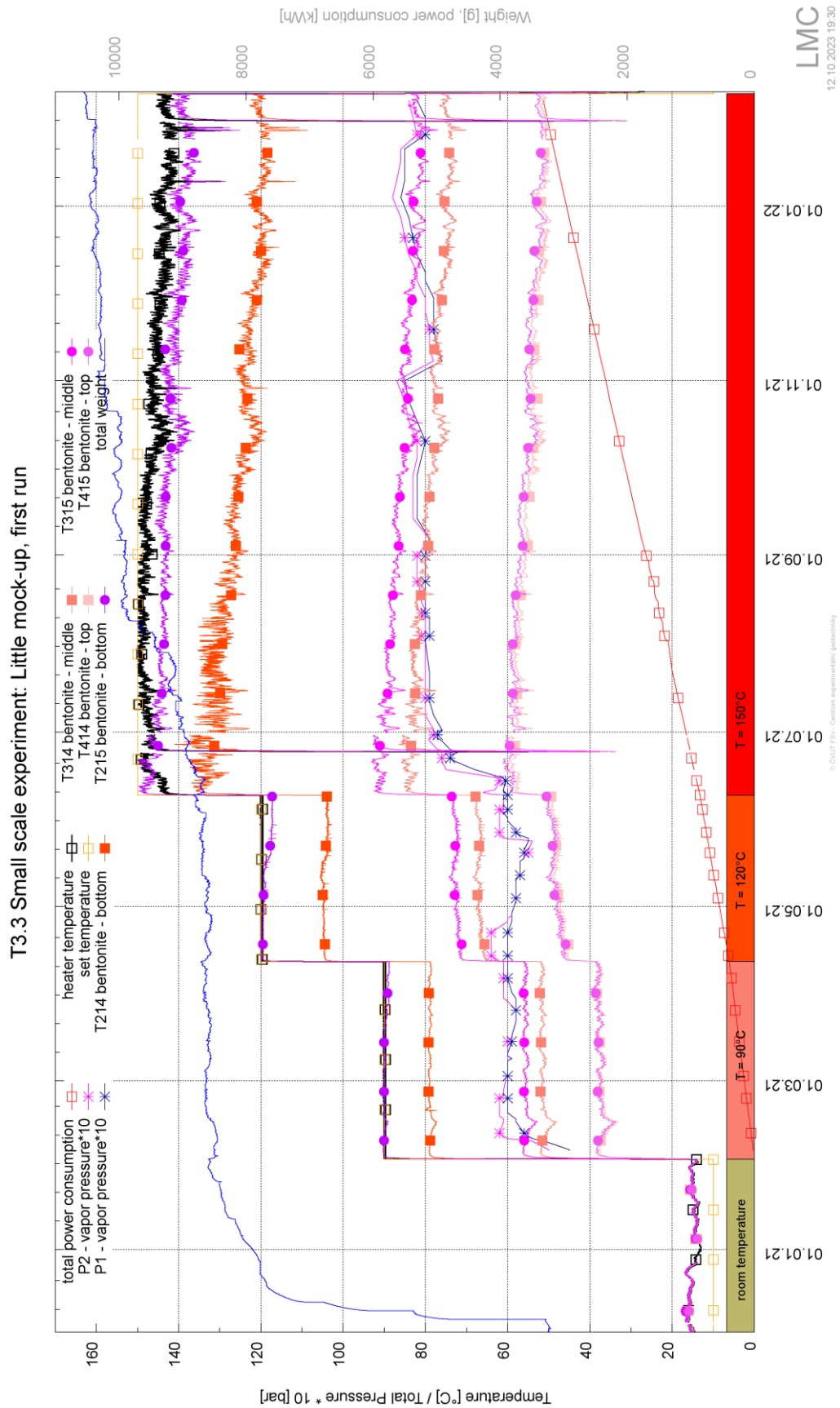


Figure 3-5. Evolution of parameters of medium-scale laboratory experiment – Test 1 (powder)

Due to its low dry density, the bentonite was fully saturated at the end of the test. This corresponds to a degree of saturation close to one throughout the profile. Samples were taken at six distances from the heater, evenly distributed over the height of the vessel, with several samples taken in each layer. The sampling scheme for each sampling profile is shown in *Figure 3-6*. A higher dry density was observed at the bottom of the experiment, near the heater, while a lower dry density was determined below the cover. The bentonite was homogeneous in each layer and no dependence on the sampling position within the layer was observed. *Figure 3-7* shows the distribution of saturation and dry density as a function of distance from the heater.

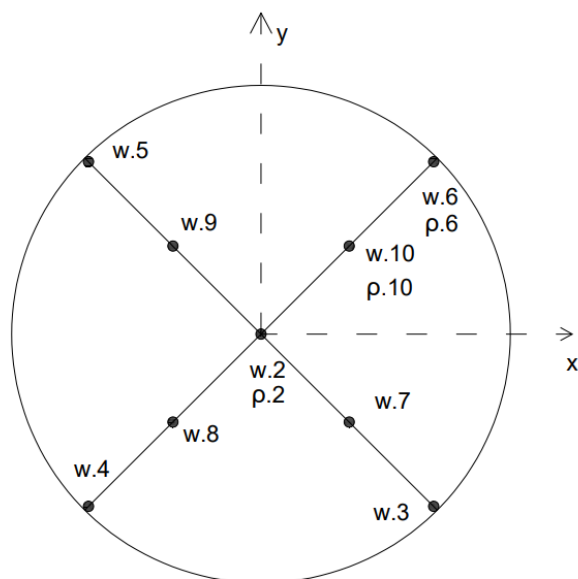


Figure 3-6 Sampling plan for dismantling of Test 1

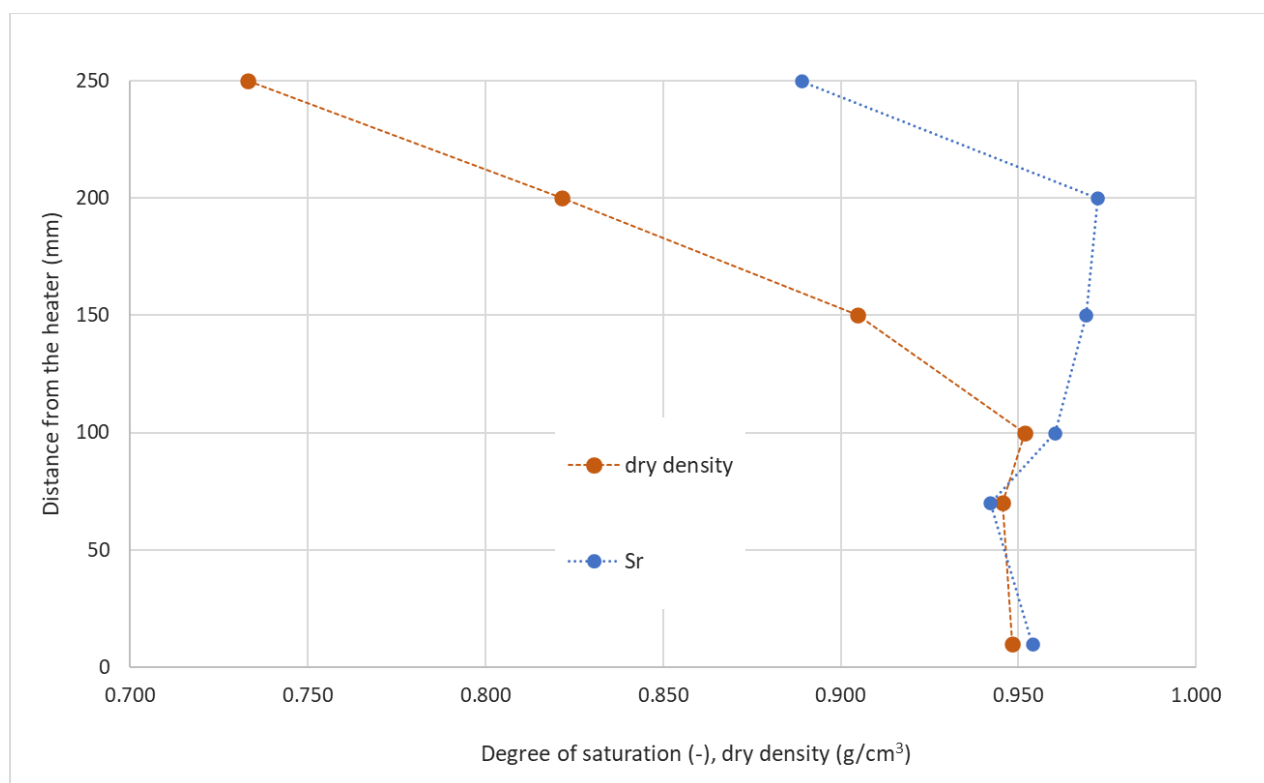


Figure 3-7. Distribution of dry density and degree of saturation as a function of the distance from the heater at the end of Test 1

Samples to analyse the hydromechanical properties and their variations due to the conditions to which the bentonite was exposed in the experiment were also taken during the sampling campaign. Specifically, hydraulic conductivity, swelling pressure and liquid limit were analysed. The findings and a comparison with the unaffected bentonite are presented in D7.7.

3.3.2 Test 2 – bentonite pellets

In the second test, pelletized bentonite BCV was used. The aim was to achieve the maximum possible compaction of the bentonite using a manual compactor. The resulting dry density was 1408 kg/m³.

The heating and saturation processes, and their order, were different in the second test compared to the first. In Test 2, the bentonite was first heated at 150°C and then saturated after the temperature field had stabilised (after 14 days). The experiment was continued for 8 months with simultaneous heating at 150°C and saturation, which corresponds to the evolution of the saturation vapour pressure, which increased continuously up to 4 bar. The evolution of measured parameters is shown in *Figure 3-8*. 80% of the total water entered the bentonite during the first 2 months, the slope of the sum curve, which expresses the amount of water entering the experiment, then flattens out and the increase of water that would contribute to the saturation of the bentonite inside the vessel approaches zero.

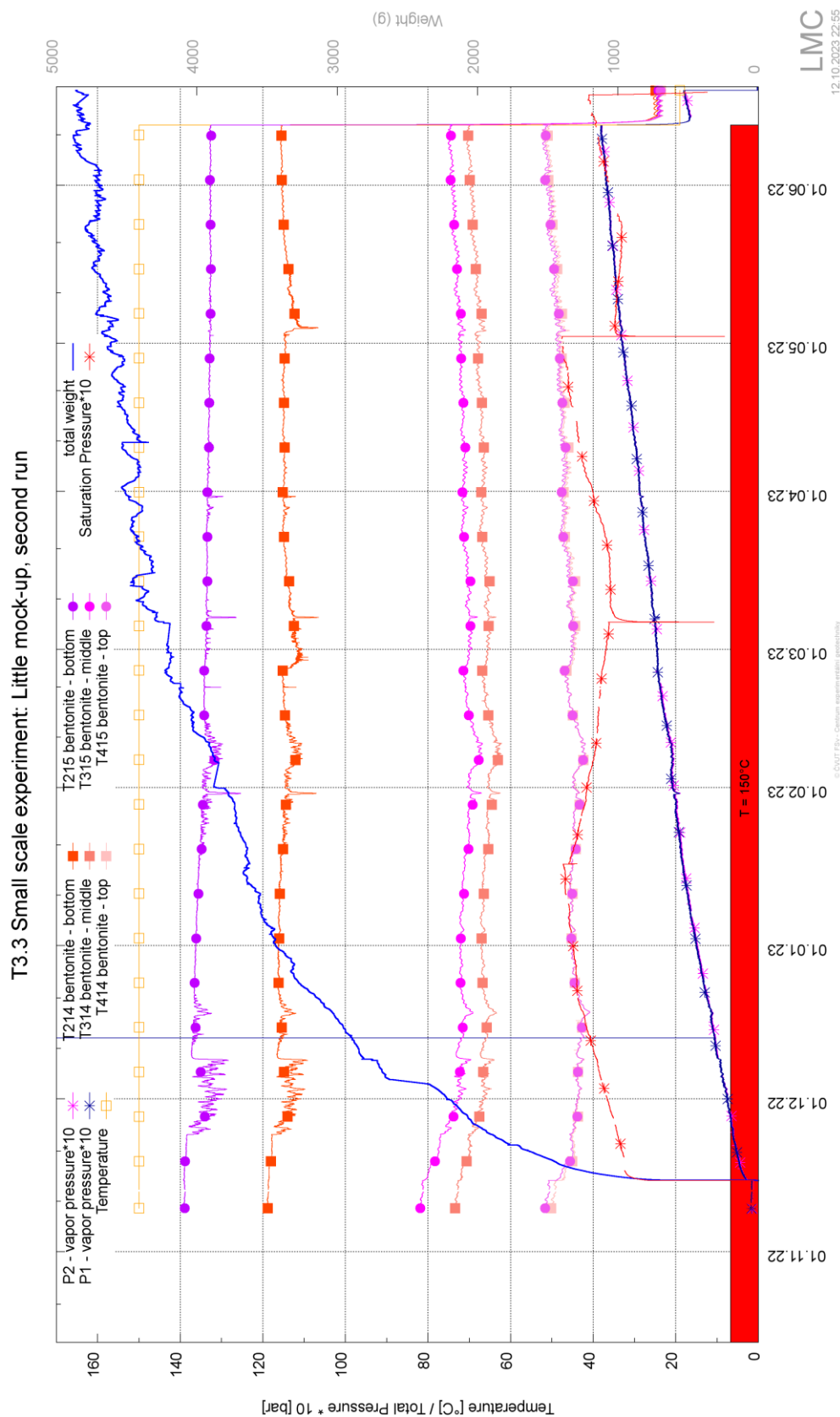


Figure 3-8. Evolution of parameters of medium-scale laboratory experiment – Test 2 (bentonite pellets)

After dismantling, samples were taken, and the water content and dry density were determined immediately. The degree of saturation was then determined from these parameters. The sampling

locations were chosen slightly differently from the first test, in two perpendicular directions, on the assumption that the system was symmetrical. *Figure 3-9* shows a schematic of the sampling plan. As in the first test, six sampling profiles were evenly distributed over the height of the experiment.

Figure 3-9 shows the sampling points from which water content and dry density were determined. The samples were taken from the surface, then 50 mm below the surface, 100 mm, 150 mm, 200 mm, 235 mm and from the bottom, above the heater. Distribution of final water content as a function of the distance from the heater and distance from the centre is shown in *Figure 3-10*. From the water content and dry density measured at the sampling points, the degree of saturation was determined and is shown in *Figure 3-11* as a function of distance from the heater and distance from the centre of the vessel.

The bentonite with the highest degree of saturation was located at the top of the vessel, farthest from the heater. Conversely, the bentonite with the lowest degree of saturation, close to zero, was located close to the heater. After eight months of saturation of bentonite pellets at a saturation pressure of 4 bar and simultaneous heating to 150°C, the upper 50 mm is saturated, the degree of saturation is about 1 and then it decreases to 0.03 in the lower part, near the heater. The graph also shows an uneven saturation of the bentonite, with moisture moving faster along the walls of the vessel. There is a higher degree of saturation at the edges of the test and a decrease towards the centre.

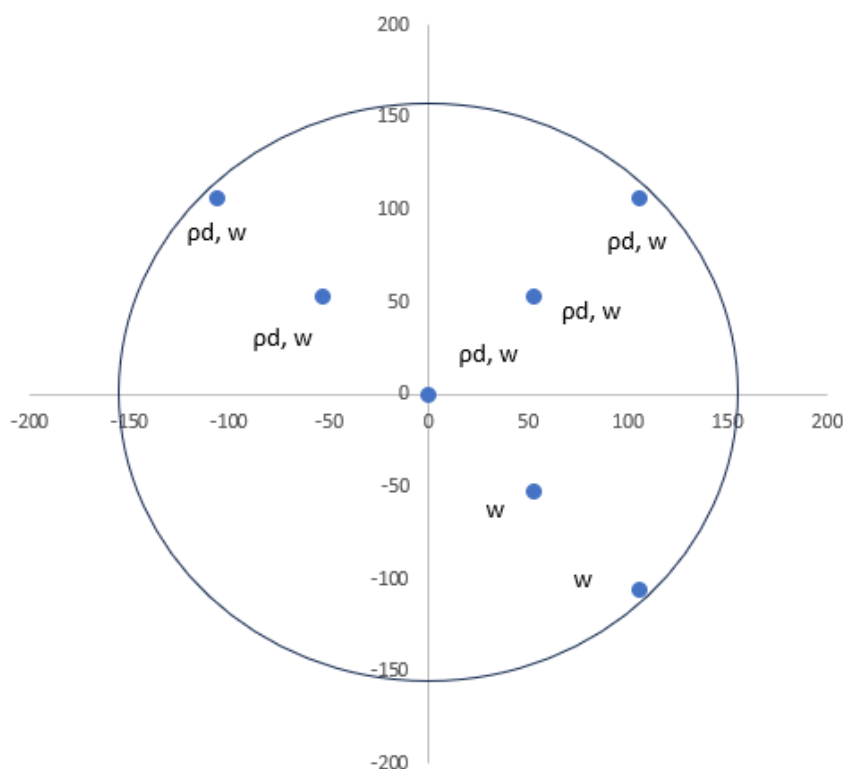


Figure 3-9. Sampling points for the determination of water content and dry density in layers of Test 2

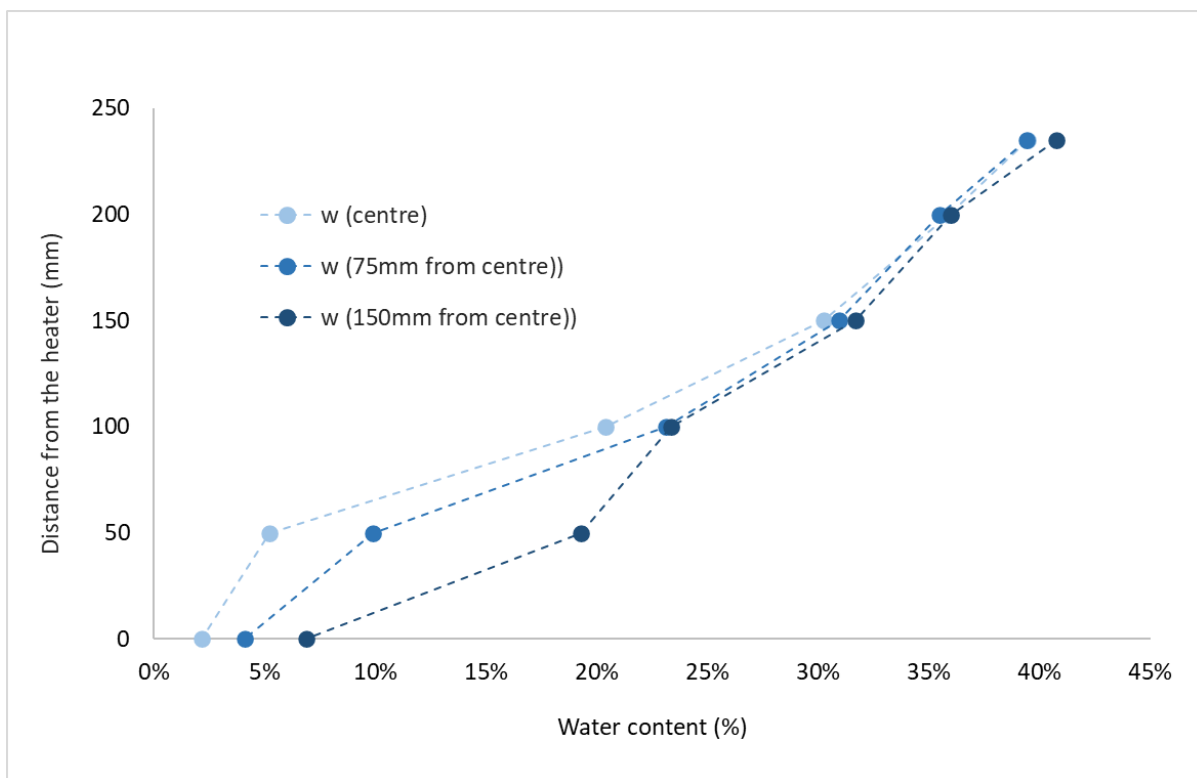


Figure 3-10. Distribution of final water content as a function of the vertical distance from the heater at each sampling point from the centre through the middle (75 mm from centre) to the edge (150 mm from the centre) in Test 2

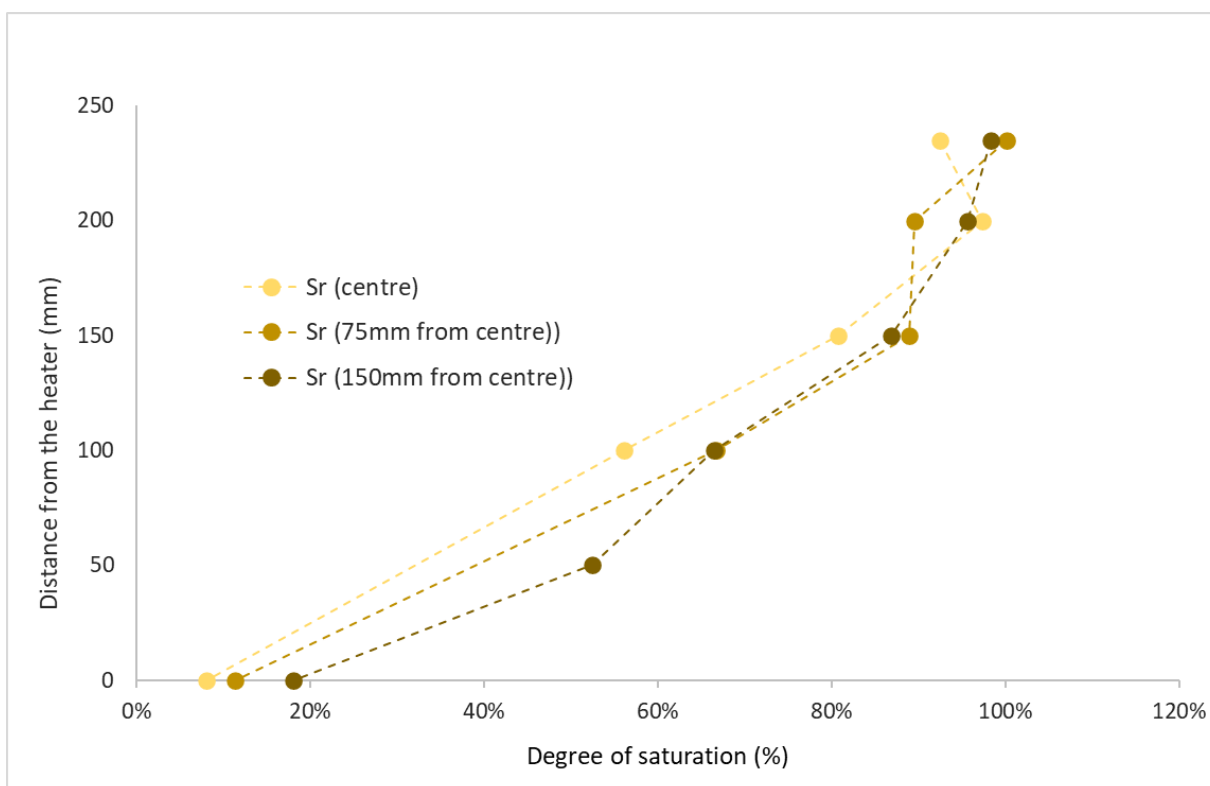


Figure 3-11. Distribution of final degree of saturation as a function of the distance from the heater at each sampling point from the centre through the middle (75 mm from centre) to the edge (150 mm from the centre) in Test 2

Figure 3-12 shows the distribution of dry density as a function of vertical distance from the heater. The graph shows the dry density at each sampling point related to the centre. Dry density was between 1260 – 1430 kg/m³. No dependence of the dry density on the distance from the centre of the experiment was observed. The dry density towards the heater increases up to a level 100 mm from the heater where a break occurs, and the dry density starts to decrease.

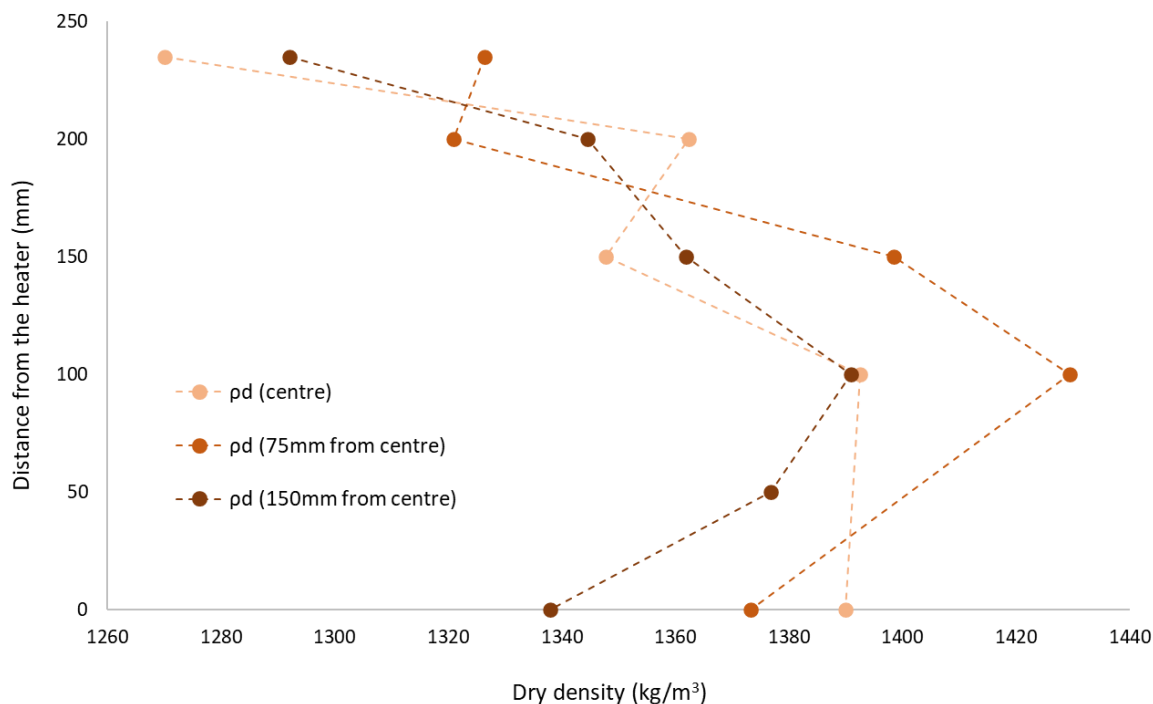


Figure 3-12 Distribution of final dry density as a function of the distance from the heater at each sampling point from the centre through the middle (75 mm from centre) to the edge (150 mm from the centre) in Test 2

Figure 3-13 shows the average dry density and degree of saturation of the whole layer depending on the distance from the heater. The graph is based on the average value of these characteristics from all sampling points in each layer. The average dry density calculated from all sampling points was 1360 kg/m³.

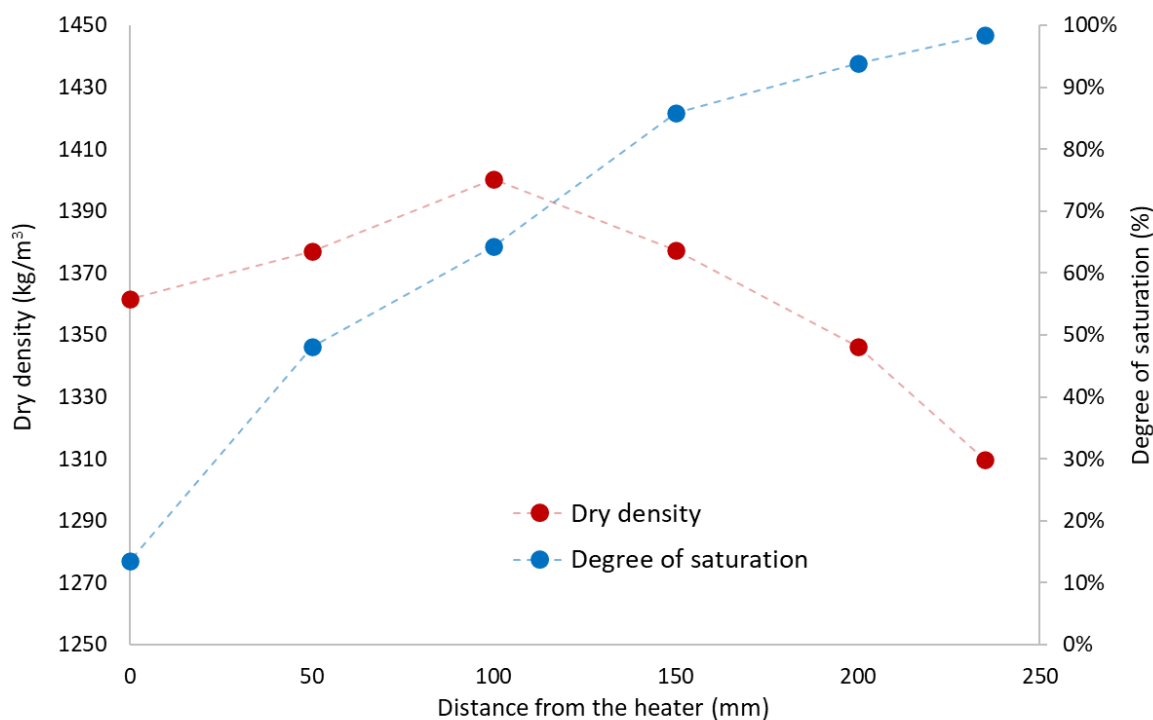


Figure 3-13. Average final dry density and degree of saturation in each layer in Test 2 (pellets)

3.3.3 THM analysis

Figure 3-14 and Figure 3-15 show a comparison of the temperature behaviour in bentonite when using bentonite powder and bentonite pellets. Figure 3-14 shows the temperature curve from a monitoring point near the centre of the experiment (60 mm from the centre, 90 mm from the edge of the vessel). Figure 3-15 shows the temperature curve at the second monitoring point, which was further away from the centre, 120 mm, 30 mm from the edge of the vessel. The temperature curves using both pellets and powder are comparable. The largest temperature difference is in the centre of the vessel, 10°C. This difference is due to the different degrees of saturation of the different forms of bentonite. While the bentonite powder was fully saturated at this point, the bentonite pellets were only 60% saturated and heat transfer was not as good as in the previous case. At the top of the vessel, both materials were fully saturated and the temperatures at this point were comparable. The bentonite pellets compensate for the temperature loss in the middle of the vessel due to their higher bulk density. The largest difference was observed at the bottom of the vessel where there was a rapid drop in temperature. This drop was due to the effect of the much lower ambient temperature as this thermometer was close to the edge of the vessel.

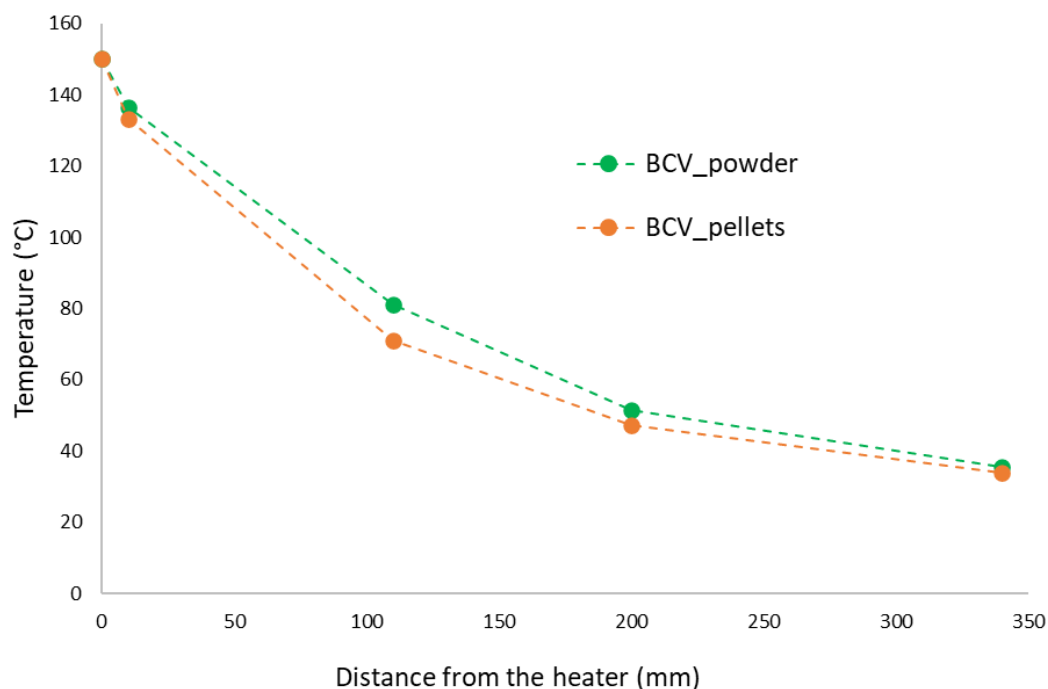


Figure 3-14. Temperature inside the bentonite as a function of the distance from the heater and on the lid. Comparison of temperature evolution with powdered bentonite and pellets. Thermometer record 60 mm from the centre of the experiment – slight influence of ambient temperature. Room temperature: 18.8°C

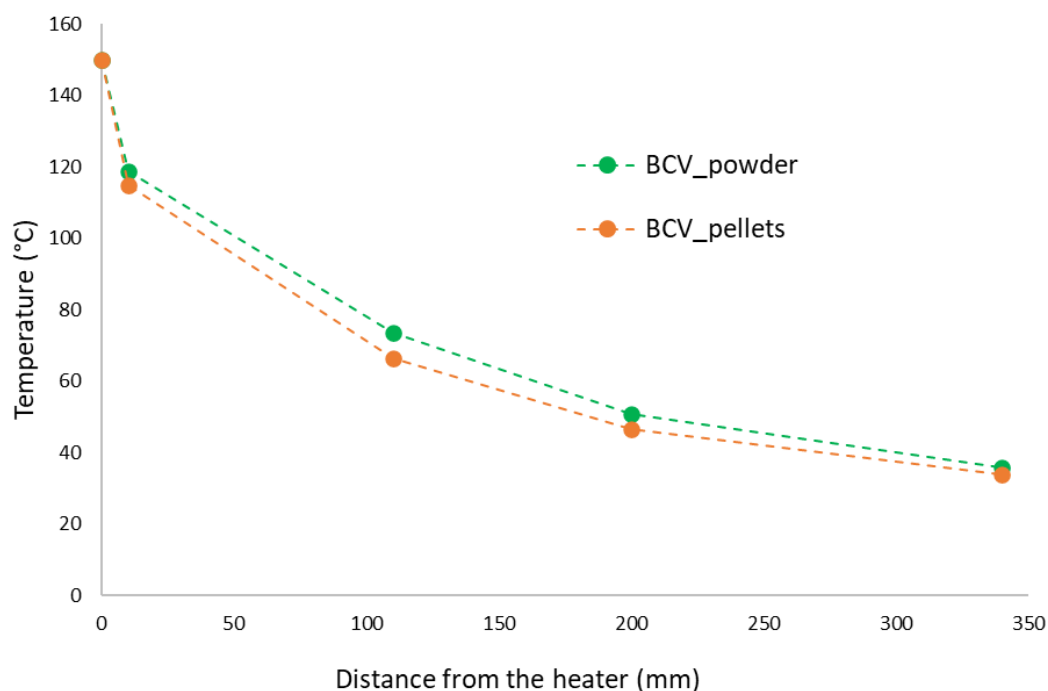


Figure 3-15. Temperature inside the bentonite as a function of the distance from the heater and on the lid. Comparison of temperature evolution with powdered bentonite and pellets. Thermometer record 120 mm from the centre of the experiment – Edge of the experiment, significant effect of ambient temperature. Room temperature: 18.8°C

Figure 3-16 shows a comparison of the degree of saturation of bentonite pellets and bentonite powder after dismantling, while the bentonite powder was fully saturated, the degree of saturation of the bentonite pellets was distributed in the vessel from the lowest, near zero, close to the heater, to the full

saturation at the top. The duration of the saturation was different, while bentonite powder was saturated for 12 months, bentonite pellets were saturated for 8 months. Given that 80% of all water entering the experiment with bentonite pellets and 90% with powdered bentonite entered during the first two months, the difference in duration of the experiment should not have a significant effect on the moisture distribution in Test 2 with bentonite pellets. Water uptake by the bentonite pellets was minimal towards the end of the experiment.

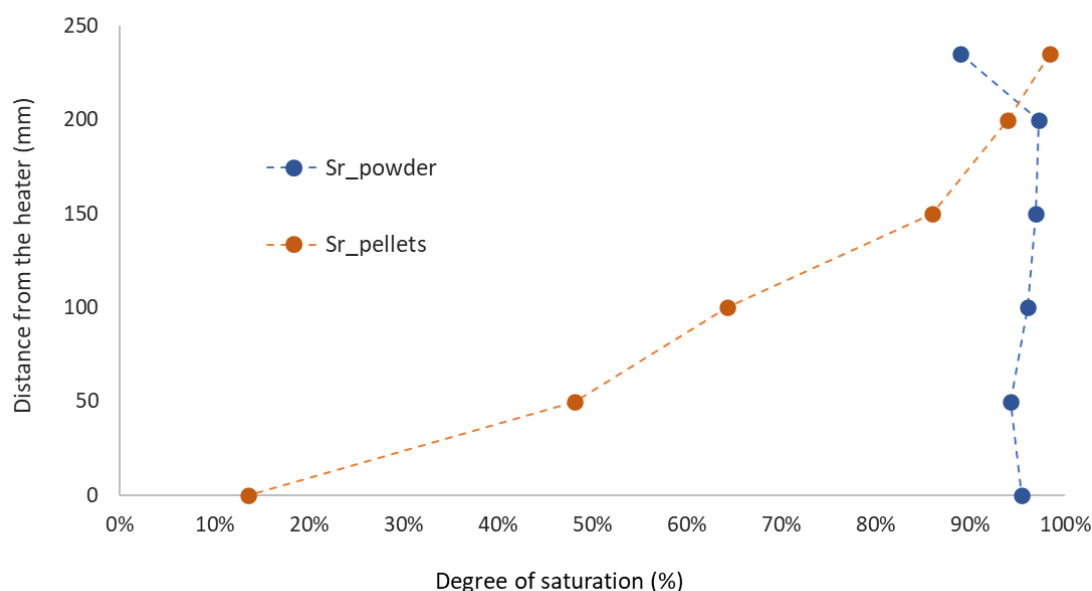


Figure 3-16. Comparison of the degree of saturation at the end of Test 1 (powdered bentonite with a dry density of 940 kg/m^3) and Test 2 (pelletized bentonite with a dry density of 1408 kg/m^3)

Results of hydraulic conductivity, swelling pressure, and liquid limit

Samples were also taken during dismantling to analyse the hydromechanical properties and their changes because of the experiment. Hydraulic conductivity, swelling pressure and liquid limit were tested. Samples were taken at various distances from the heater. The results are presented in detail in D7.7 in context of results of hydromechanical properties of bentonite after the laboratory treatment consisting of long-term exposure to 150°C in dry and wet moisture state. The results obtained on bentonite from the medium scale experiment are consistent with those from laboratory thermally treated bentonite and a brief description of the results follows.

The results of the experiment using powdered bentonite showed that the hydromechanical properties are stable when exposed to high temperatures in the saturated state. The bentonite in the experiment was fully saturated, even in the lower part close to the heater. Although a temperature gradient was applied in the experiment, no dependence of the THM properties on the distance from the heater was observed. The hydraulic conductivity, swelling pressure and liquid limit did not change after the experiment and were the same as in the case of untreated bentonite.

Unlike powdered bentonite, in the experiment where pellets were used the hydromechanical properties of bentonite were already affected due to the moisture condition in which the bentonite was exposed to elevated temperature. In Test 2, the bentonite was compacted to a higher dry density and therefore the bentonite was not fully saturated. As a result, the bentonite was unevenly saturated and was exposed to elevated temperature in the dry condition at the bottom of the vessel, near the heater. The samples taken near the heater had a higher hydraulic conductivity and lower liquid limit than unaffected bentonite

pellets. These results are also consistent with those obtained on laboratory treated bentonite, where dry treated bentonite was tested. Swelling pressure was not affected.

In the case of exposure to high temperatures, it does not matter whether it is pellets or powder, the more important influence is the moisture state in which the bentonite is exposed to the elevated temperature.

3.4 Conclusion

Two medium-size experiments were carried out as part of subtask T3.3. The tests consisted in placing the bentonite in a vessel and then heating the bentonite with a heater at the bottom of the sealed vessel while saturating it through the lid. This created a temperature gradient in the vessel. This experiment simulated, on a small scale, the conditions in a waste repository: saturation of the barrier on one side and heating on the other. BCV bentonite powder was used in the first experiment and BCV bentonite pellets in the second one. While the bentonite powder was completely saturated after the experiment, the moisture in the bentonite pellets was heterogeneously distributed. This was due to the lower dry density of the bentonite powder, which was 940 kg/m^3 and to the testing procedure. The dry density of the bentonite pellet test was 1408 kg/m^3 . The bentonite in the first experiment (powder) was exposed to elevated temperature from the start in the saturated state. In the second experiment (pellets), the heat source was applied to the dry bentonite, which was simultaneously saturated. At the bottom of the vessel, close to the heat source, the bentonite was dry after the experiment and the degree of saturation increased with distance from the heater until full saturation was reached at the surface. The addition of water to the experiment was minimal after 8 months, which together with the progression of saturation indicates the formation of a plug in the upper layer near the water source. The results of the postmortem hydromechanical behaviour analyses are consistent with the results of T3.1. While the hydromechanical characteristics of the bentonite that was heated in the saturated state did not change and were consistent with the untreated bentonite, the characteristics of the bentonite from the second test taken near the heater deteriorated in terms of an increase in hydraulic conductivity and a decrease in the liquid limit. The swelling pressure was not affected by the thermal treatment.

4. Summary and conclusions

The description of the test performed in Subtask 3.3 by CIEMAT and CTU and the results obtained have been reported. They were thermo-hydraulic tests intended to simulate the conditions of the bentonite buffer in the repository. Namely two kinds of tests were performed:

3. hydration tests under thermo-hydraulic gradient (TH tests), and
4. hydration tests under high isothermal temperature.

The first group of tests, in which the buffer material is simultaneously submitted to thermal and hydraulic gradients, aims to simulate the conditions of the whole barrier during operation, where the temperatures may be significantly different from those areas closest to the canister to those at the host rock contact. These tests were performed by CIEMAT and CTU, using different materials, cell dimensions, initial buffer conditions and testing protocols. The main features of each of these tests are given in *Table 4-1*. The tests can be considered medium-scale ones, since their dimensions are relevant for the usual barrier thickness envisaged by most repository concepts. In all of them the heater plate simulating the canister surface was placed at the bottom (at temperatures 140-150°C) and the temperature on top was regulated either at 20°C or at room temperature. Hydration water was supplied through the top at a low injection pressure. Out of the TH tests included in this Subtask, test HEE-B reproduced the conditions of a large-scale in situ experiment (HE-E at Mont Terri), whereas the others were not representative of any particular disposal concept.

Table 4-1. Summary of the TH performed in Subtask 3.3

| Test ref. | Material | Buffer h $\times \phi$ (cm) | Initial ρ_d (g/cm ³) / w (%) | Heater T (°C) | Hydration water | Test sequence | Duration (months) |
|-----------------|------------------------|----------------------------------|--|--------------------|--------------------|----------------------------|----------------------|
| CIEMAT HEE-B | MX-80 pellets | 50 x 7 | 1.53 / 6 | 140 | Pearson | 1. Heating 2. Hydration | 120 |
| CIEMAT HT1 | Compacted Bara-Kade | 10 x 10 | 1.55 / 17 | 150 | Glacial | 1. Heating 2. Hydration | >32 |
| CIEMAT HT2 | Compacted Bara-Kade | 10 x 10 | 1.55 / 17 | 150 | Saline | 1. Heating 2. Hydration | 32 |
| CTU Test 1 | BCV powder | 25.5 x 30 | 0.95 / 13 | 150 | Distilled | 1. Hydration 2. Heating | 12 |
| CTU Test 2 | BCV pellets | 25.5 x 30 | 1.41 / 10 | 150 | Distilled | Simultaneous | 8 |

The second group of tests were only carried out by CIEMAT, with the aim of assessing how the high temperatures close to the heater could affect the hydration rate and swelling development. Thus, they were carried out under isothermal high temperatures (120, 140°C) with FEBEX bentonite compacted at dry density 1.6 g/cm³ with its hygroscopic water content.

Hydration under thermal gradient can progress even if the water injection pressure is very low. However, the tests reported did not allow to check if full saturation of the areas closest to the heater is possible, either because the tests were too short (CTU Test 2) or because of experimental artefacts, namely evaporation through the sensors' inlets (CIEMAT HEE-B and HT2). It is expected that test HT1 (to be dismantled before the end of the project) will provide information on this aspect, because it is running with no leaks and it will be sufficiently long to allow full saturation if the temperature of the heater were lower (this has been checked in other tests not reported here). However, relevant radial swelling stresses –associated to the increase in water content– were recorded during saturation, higher when diluted water was used instead of saline one. The infiltration tests performed under isothermal conditions

($T=120^{\circ}\text{C}$ and 140°C) also showed relevant pressure build up, although with values lower than expected for room temperature.

At the end of the tests, significant gradients in the water content and dry density distributions had been developed in the bentonite, with higher water contents close to the hydration surface, where the dry density was lower. It is worth mentioning that none of those tests had reached full saturation (only CTU Test 1 reached full saturation, but it had been fully saturated prior to heating and its dry density was very low). However, in the isothermal tests, where hydration took place through the bottom of the samples, the dry density distribution followed the opposite trend, with the lower values measured on the block side opposite to the hydration surface, where also the highest water contents were measured. This distribution likely results from the upwards vapour movement, which would also trigger bentonite swelling and increase in porosity.

The tests performed with pellets showed trends of behaviour similar to those expected for compacted bentonite.

Overall, these conclusions and the knowledge gained are not different from those that had been reached in previous projects for lower temperatures.

References

1. Gaus, I., et al., *The HE-E Experiment: Lay-out, Interpretation and THM Modelling.*, in *Nagra Arbeitsbericht 2014*, NAGRA: Wettingen. p. 140.
2. Plötze, M. and H.P. Weber, *ESDRED: Emplacement tests with granular bentonite MX-80.*, in *Nagra Arbeitsbericht 2007*, Nationale Genossenschaft für die Lagerung radioaktiver Abfälle (NAGRA): Wettingen. p. 73.
3. Villar, M.V., *Long-term THM tests reports: Isothermal infiltration tests with materials from the HE-E. PEBS Deliverable 2.2-7.2.*, in *CIEMAT Technical Report 2013*, CIEMAT: Madrid. p. 32.
4. ENRESA, *FEBEX Full-scale Engineered Barriers Experiment, Updated Final Report 1994-2004*. Publicación Técnica ENRESA Vol. 05-0/2006. 2006, Madrid: ENRESA. 590.
5. Villar, M.V. and R. Gómez-Espina, *Report on thermo-hydro-mechanical laboratory tests performed by CIEMAT on FEBEX bentonite 2004-2008.*, in *Informes Técnicos CIEMAT*. 2009, CIEMAT: Madrid. p. 67.
6. Villar, M.V., et al., *THM cells for the HE-E test: setup and first results. PEBS Deliverable 2.2-7.1.*, in *Technical Report CIEMAT*. 2012, CIEMAT: Madrid. p. 34.
7. Villar Galicia, M.V., R.J. Iglesias Martínez, and C. Gutiérrez-Álvarez, *THM column cell with MX-80 pellets simulating the HE-E in situ experiment for 10 years: online results and final physical state*, in *Informes Técnicos Ciemat*. 2022, CIEMAT: Madrid. p. 65.
8. Idiart, A., et al. *Laboratory experiments of thermo-hydro-geochemical evolution of compacted bentonite*. in *7th International Conference on Clays in Natural and Engineered Barriers for Radioactive Waste Confinement*. 2017. Davos.
9. Garitte, B., et al., *DECOVALEX-2015: A THM modelling benchmark based on the performance of heated and hydrated granulated bentonite mixture column tests.* , in *6th International Conference Clays in natural and engineered barriers for radioactive waste confinement.* . 2015: Brussels. p. 144.
10. Villar, M.V., et al., *Heating and hydration of a column of bentonite pellets for 10 years: postmortem characterisation*, in *Informes Técnicos CIEMAT*. 2023, CIEMAT: Madrid. p. 85.
11. Villar, M.V. and A. Lloret, *Influence of temperature on the hydro-mechanical behaviour of a compacted bentonite*. *Applied Clay Science*, 2004. **26**(1-4 SPEC. ISS.): p. 337-350.
12. Hausmannová, L., I. Hanusová, and M. Dohnáková, *Summary of the research of Czech bentonites for use in the deep geological repository – up to 2018*. 2018, Prague: SÚRAO.
13. Červinka R., V.R.e.a., *Kompletní charakterizace bentonitu BCV 2017*. 2018, Prague: SÚRAO.
14. Svoboda J., V.R., et al., *Interakční experiment – přípravné a podpůrné práce*. 2019, Prague: SÚRAO.